BACTERIOPHAGE: A POTENTIAL TREATMENT FOR CITRUS CANKER

A Thesis

by

TRAM THI BICH LE

Submitted to the Office of Graduate and Professional Studies of
Texas A&M University
in partial fulfillment of the requirements for the degree of

MASTER OF SCIENCE

Chair of Committee,	Carlos F. Gonzalez
Committee Members,	Jason J. Gill
	Leland S. Pierson III
Head of Department,	Leland S. Pierson III

August 2019

Major Subject: Plant Pathology

ABSTRACT

Citrus canker, caused by *Xanthomonas axonopodis* pv. *citri* (*Xac*), is one of the most devastating citrus diseases that affects citrus production worldwide. The current recommended means to control canker are windbreaks, copper sprays, and control of leafminer, its insect vector, with copper sprays being most effective. However, there is growing concern about the buildup of copper in groves leading to phytotoxicity, decreased plant productivity, copper resistance development, and copper contamination of ground and river water. The goal of this study was to develop a non-copper based treatment for citrus canker. Using virulent bacterial viruses (phages) that specifically targeted to *Xac* is an approach that is not harmful to humans, animals, plants, associated beneficial microflora, or the environment. I report here the isolation and characterization of three virulent phages for *Xac* that differ in host range and morphology. Genomic analysis showed that CCP504 is a phiKMV-like phage, CCP513 is a novel siphophage, and CCP509 is a T4-like phage type, respectively. All three phages appear to utilize type IV pili as their primary receptors for adsorption. Greenhouse studies were conducted to evaluate the efficacy of phage therapy to control canker formation on Hamlin sweet oranges using a phage cocktail composed of three KMV-like podophages (CCP504, CCP505 and CCP511) and one siphophage (CCP513). Both pre- and post-treatments with this phage cocktail at an MOI of 20 resulted in a significant reduction in lesion formation on leaves of the treated plants as compared to non-treated plants. My research demonstrates that bacteriophages can serve as an alternative control strategy for *Xac* that is both environmentally friendly and sustainable.

ACKNOWLEDGEMENTS

I would like to thank my committee chair, Dr. Gonzalez, and my committee members, Dr. Gill and Dr. Pierson for their guidance and support throughout the course of this research.

I would like to thank Dr. Jinyun Li and Dr. Nian Wang at University of Florida for their assistance in conducting the greenhouse experiments.

I would like to thank Guichun Yao for her continuous support, Drs. Aravind Ravindran and Mayukh Das, and Karl Gorzelnik for their advice and assistance. Thanks also go to my friends and colleagues in Dr. Gill's laboratory, Center for Phage Technology and Ran Meng in Dr. Zhang's lab for their support, and the Department of Plant Pathology and Microbiology faculty and staff for making my time at Texas A&M University a great experience.

I would like to thank my friends and family here in America and back home in Viet Nam for their continuous love and support through my journey.

Finally, I want to extend my gratitude to Citrus Research and Development Foundation and Otsuka Pharmaceutical Co. Ltd. for providing funding sources for my research.

CONTRIBUTORS AND FUNDING SOURCES

Contributors

This work was supervised by a thesis committee consisting of Professor Carlos F. Gonzalez [Advisor] and Professor Leland S. Pierson III of the Department of Plant Pathology and Microbiology [Home Department] and Assistant Professor Jason J. Gill of the Department of Animal Science [Outside Department].

The efficacy study of phage cocktail in greenhouse trials for Chapter IV was conducted in collaboration with Dr. Jinyun Li and Dr. Nian Wang from University of Florida Citrus Research and Education Center in Lake Alfred, FL.

All other work conducted for the thesis was completed by the student independently.

Funding Sources

Graduate study was supported by Citrus Research and Development Foundation and Otsuka Pharmaceutical Co. Ltd.

TABLE OF CONTENTS

Page

LIST OF FIGURES

Page

LIST OF TABLES

Page

CHAPTER I

INTRODUCTION AND LITERATURE REVIEW

The pathogen

Xanthomonas axonopodis pv. *citri (Xac)* is a rod-shaped Gram-negative bacterium with a single polar flagellum (Agrios, 1997). It is the causal agent of citrus canker, a disease that affects citrus production worldwide (Gottwald et al., 2002). The pathogen causes distinct raised necrotic lesions on leaves, stems, and fruits. Severe infections can lead to defoliation, blemished fruit, premature fruit drop, twig dieback, and general tree decline (Schubert et al., 2001). It can cause serious damage to all citrus cultivars and some citrus relatives, but is not harmful to humans or animals (Dewdney et al.). The Asiatic type of canker (Canker A), caused by *Xac*, is the most widespread and causes the most severe form of the disease, whereas the cancrosis B and C caused by *X. axonopodis* pv. *aurantifolii* (Graham et al., 2004) are less severe. The canker A-strain is most severe on grapefruit, some sweet oranges Hamlin, Pineapple and Naval, Mexican (Key) lime, and the hybrids of trifoliate orange used for rootstocks. The cancrosis B-strain is most serious on lemons and also infects Mexican lime, sour orange and pummelo. The C-strain is only present in Brazil and infects Mexican (Key) lime (Graham et al., 2004; Schubert et al., 2001). In nature, the canker A-strain gradually supplants and dominates over the B-strain, when both are present. More recently, primers based on sequence differences in 16S-23S internally transcribed spacers (ITS) and the plasmid gene *pthA* were developed to differentiate between the A, B and C-strains (Cubero and Graham, 2002).

Xac produces abundant extracellular polysaccharide (EPS) and xanthan that encapsulates bacterial cells in the late logarithmic and stationary growth phases, which contribute to inoculum survival (Goto and Hyodo, 1985). Pathogenicity factors such as type III secretion systems (T3SS) and the effector gene for pathogenicity (*pthA*) are critical for the development of citrus canker symptoms (Das, 2003). PthA is translocated into host cells via T3SS and its expression is sufficient for symptoms (hypertrophy, hyperplasia and cell death) that are diagnostic of citrus canker disease (Duan et al., 1999). In *Xac*, production of virulence factors is controlled by a cluster of regulation of pathogenicity factors (*rpf*) that encoded elements of a cell-cell communication system called quorum sensing (QS) (Barber et al., 1997). The QS regulatory system of *Xac* is mediated by a diffusible signal factor (DSF) (Ryan et al., 2011; 2015). The DSF-mediated QS in *Xac* influences the synthesis of extracellular enzymes such as endoglucanase, protease, and endomannanase, and the xanthan EPS, as well as alterations in biofilm formation that assists in egression of the pathogen from the canker lesion (Brunings and Gabriel, 2003; Li et al., 2019). Once within the apoplastic space, the bacteria adheres to the host cell wall surfaces via the hypersensitive reaction and pathogenicity (hrp) pili (He, 1998) or type IV pili (T4P) (Brunings and Gabriel, 2003). *Xac* can also manipulate host responses via a plant natriuretic peptide (PNP)-like protein (XacPNP). The XacPNP acts to improve host photosynthesis, which results in more new tissue growth during infection. This regulation of host development suits the biotrophic lifestyle of *Xac* and prolongs its survival (Gottig et al., 2010).

Xac is not a systemic pathogen, however all tissues above ground are susceptible to *Xac* infection, with young tissue being most susceptible (Schubert and Miller, 1996;

Schubert et al., 2001). The optimum temperature for infection is between 20 and 30ºC (Koizumi and Kochinotsu, 1977). Under less than ideal infection and incubation conditions, symptoms may take up to two months or more to be noticeable (Schubert et al., 2001). An inoculum source for young exposed tissue on the same plant or new plants is bacterial ooze from lesions containing high concentrations of biofilm-coated aggregates of *Xac* (Timmer et al., 1991). *Xac* survives primarily and seasonally within the margins of the lesions. Outside of the lesions, *Xac* only survives 1-3 days on inanimate surfaces, such as agricultural equipment and clothing, and no more than two months in soil due to antagonism and competition with saprophytes (Graham et al., 1989; Schubert et al., 2001). *Xac* infections occur primarily through stomates and wounds produced via wind-driven rain and by insects (Das, 2003). Another factor that can exacerbate the incidence and severity of citrus canker is larval feeding by Asian citrus leaf miner (CLM; *Phyllocnistis citrella*) (Belasque Jr et al., 2005). The disease life cycle of citrus canker is shown in Figure 1.

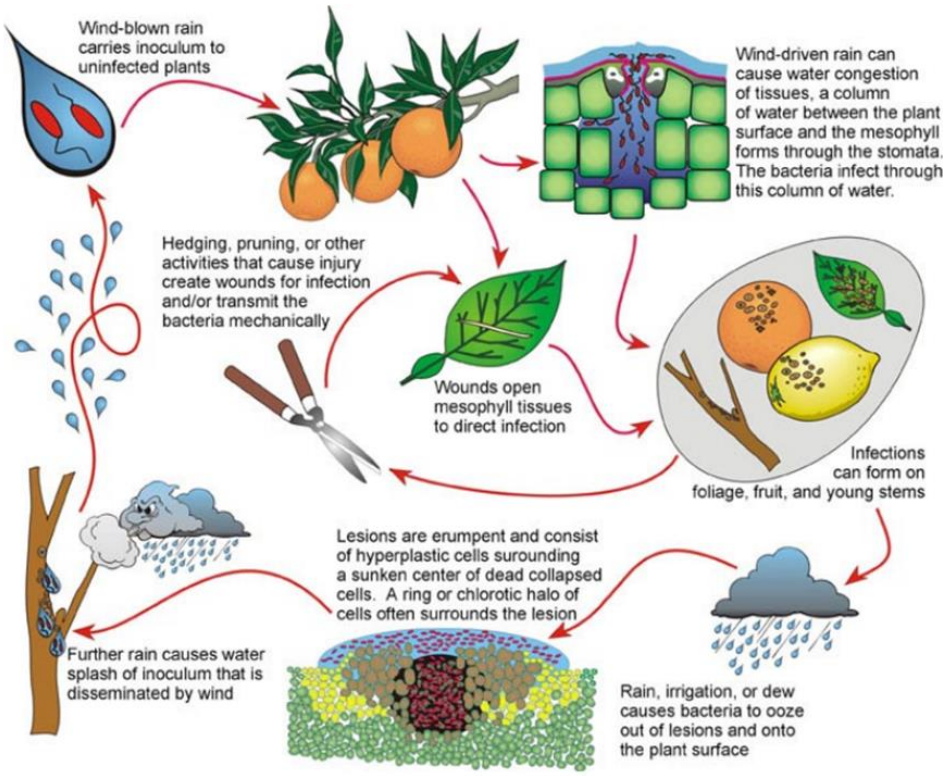

Figure 1. The disease cycle of citrus canker (Figure adapted from Schubert et al., 2001).

Economic impact

Citrus canker continues to be a potential threat to worldwide citriculture (Das, 2003). The disease is thought to have originated in southeastern Asia or India and spread through much of Asia, to Japan, southern and central Africa, the Middle East, Australia, New Zealand, the Pacific Islands, South America and the southeastern United States of America (Schubert and Miller, 1996). In the United States, Florida has greater than 150-year history of citrus production and produces three quarters of total US citrus (Zhou et al., 2011). Canker has become endemic in Florida since the end of a state/federal eradication program in January of 2006 due to the failure of this program (Gottwald and Irey, 2007).

From 1996 through late 1999, the up-front costs of the eradication program increased from approximately $10 million to $50 million/year. In 2000-2001, an all–out eradication program was put in place against further spread of the disease, which increased the expense up to $200 million dollars (Schubert et al., 2001). Table 1 shows the statistical data of the citrus canker eradication program in the areas affected by this disease in Florida as of January 2001.

Table 1. Citrus Canker Eradication Program statistics in the geographic areas where citrus canker occurred in FL, January 2001 (Schubert et al., 2001).

Geographic area (counties)	**Quarantines area(s) (no.)**	**Quarantine area(s) (mi^2)**	**Residential trees removed**	**Commercial trees removed**
Southeast FL (Dade, Broward, Palm Beach)	1	1,000	568,807	290,718
Southwest FL (Hendry, Collier)	6	159	2,299	532,281
West central FL (Manatee, Hillsborough)	3	162	5,144	100,811
Total	10	1,321	576,250	923,810

In addition to threatening the growth and survival of citrus, the disease makes fruits unappealing and unmarketable. Twig dieback, fruit blemish, and early fruit drop, which occur during the advances stages of the disease, have major economic impacts (Schubert et al., 2001). Even with current control measures in place, estimates from studies in South America show fresh fruit crop losses at $80 to $160/acre/year for early oranges, $31 to $79/acre/year for mid-season oranges, and $69 to $137/acre/year for grapefruit (Schubert et al., 2001).Furthermore, there has been a decline of 32.7% in value of sale from a high of $1.1 billion in 1999-2000 to $746 million in 2004 (Goodwin and Piggott, 2006). More

recent economic impact analysis showed that grapefruit, Florida's most important fresh fruit species, is declining in value. In 2005-2006, grapefruit was valued at $174 million, but by the 2009-2010 crop year, it had experienced a 30% decrease in value; it was worth only $123 million (Graham et al., 2010). This loss is due to legal restrictions preventing the packing of fruit exposed to canker, restriction of shipping to export markets, abandonment of groves due to loss of profitability, diversion of fruit to the production of juice and a decreased in consumption (Ritenour et al., 2010).

Current control measures

In countries where citrus canker has not yet occurred, control measures rely heavily on quarantine to prevent the introduction and establishment of *Xac*. In regions where canker has occurred but not yet become endemic, measures of control are focused on isolation and eradication of the pathogen, minimization of dissemination, reduction of inoculum sources, and protection of susceptible tissue from infection (Behlau et al., 2016). In regions where citrus canker has become endemic and an eradication program is no longer feasible, measures for disease management include: the planting of citrus canker-free nursery stock, the use of less susceptible citrus cultivars, the deployment of arboreal windbreaks, the treatment of plants with copper-based bactericides, the control of citrus leaf miner and the application of systemic acquired resistance (SAR) inducers (Behlau et al., 2008; Graham et al., 2010; Leite Jr and Mohan, 1990; Stein et al., 2007). Among these integrated measurements, the most common and highly effective practices are windbreak and copper spray (Gottwald and Timmer, 1995; Moschini et al., 2014). The effectiveness of copper bactericides for citrus disease control has been comprehensively evaluated over the last three decades. Recent research show that successful management of *Xac* in

endemic areas is highly dependent on copper sprays (Behlau et al., 2017). However, long-term use of copper bactericides has several disadvantages including accumulation in soil which has negative impacts on root growth and nutrient uptake by citrus trees, fruit blemishing as a result of phytotoxicity and development of copper-resistance due to the ability of *Xac* to a acquire plasmid-borne gene(s) conferring resistance in xanthomonad populations (Graham et al., 2010). Kandeler et al (1996) observed that microbial biomass, enzyme activity, and functional diversity of soil microbial communities decreased with increasing Cu pollution (Kandeler et al., 1996; Zhou et al., 2011). Furthermore, when using copper bactericides exclusively, citrus canker management on susceptible cultivars is challenging because wind-blown rain introduces *Xac* directly into stomata, bypassing the protective copper film on the plant surface (Ference et al., 2018). Thus, there is an urgent need to develop new environmentally-friendly control strategies to combat citrus canker.

Bacteriophage biology

Bacteriophages (phages) are viruses that infect bacteria, and are the most numerous and most diverse life forms on earth, estimated at 10^{31} tailed phages in the biosphere (Brüssow and Hendrix, 2002; Clokie et al., 2011). There are many different types of phages that range from double stranded DNA (dsDNA) to single stranded RNA phages. The dsDNA tailed phages have been classified into three families: *Podoviridae*, *Siphoviridade* and *Myoviridae* that belong to the order of *Caudoviridales* (‘cauda’, which is Latin for tail) which account for ~95% of all reported phages (Ackermann, 2006). Podophages have short, non-contractile tails, siphophages have long, non-contractile tails, and myophages have long contractile tails (Figure 2) (Nobrega et al., 2018). Phages depend on their host cells to produce and release new viral particles. This event can be

easily observed in laboratory conditions by the formation of plaques on lawns of susceptible bacteria or lysis of liquid cultures.

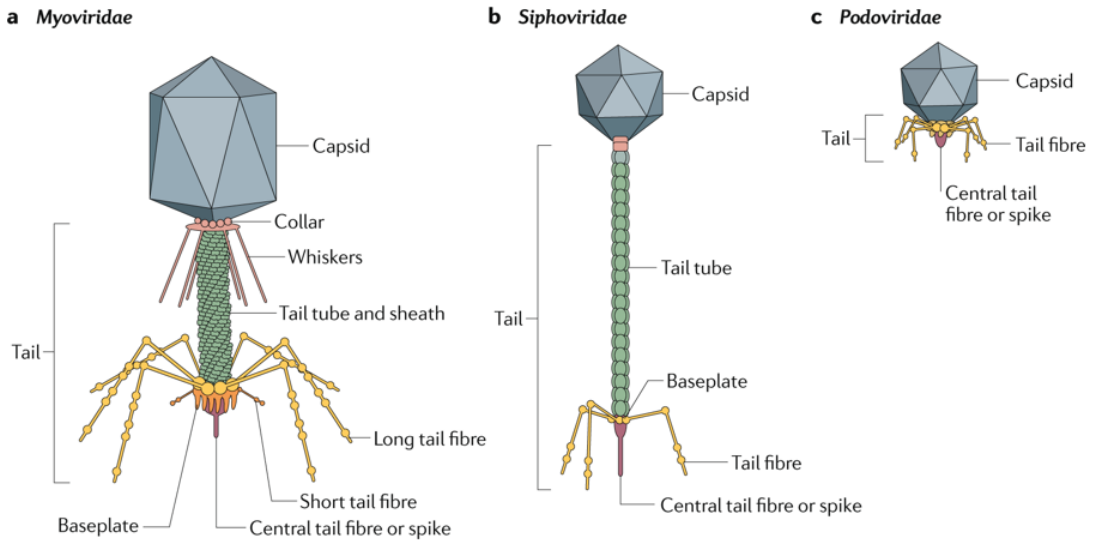

Figure 2. Double-stranded DNA tailed phages. (a) Myoviridae family (b) Siphoviridae family (c) Podoviridae family. Both siphophages and myophages have baseplates at the distal end of the tail that attach to receptor-binding proteins (RBPs), such as tail fibers and tail spikes. Podo phages do not have baseplate, therefore the RBPs attaches directly to the tail (Figure adapted from Nobrega et al., 2018, with permission).

Phages recognize and attach to specific receptors on the bacterial surface such as the liposaccharides (LPS), oligosaccharides or outer membrane proteins (Chaturongakul and Ounjai, 2014) as well as flagella or pili (Koskella and Taylor, 2018). Phage adsorption on host cell surface is a two- stage process: reversible and irreversible binding. The molecular mechanisms of interaction at both stages are specific to different phage-host systems and may vary significantly in representatives of diverse taxonomy groups. Adsorption rate is characteristic of each phage-host pair and varies depending on phage/host concentration. Injection of genetic material into the host cell takes place after

the irreversible adsorption phase. Electrochemical membrane potential, ATP molecules, enzymatic splitting of peptidoglycan layers, or all three factors may be vital for this process. Mechanisms of penetration are specific for each phage or phage groups (Rakhuba et al., 2010).

There are two known life cycles that a phage can undergo once it injects its genetic material into host cell: lytic or lysogenic (Figure 3). In the lytic life cycle, the host cell supplies the molecular building blocks and enzymes necessary for phage replication and production of new phages particles. The phage encodes proteins such as holin and endolysin to lyse host cell from within to release progeny (Doss et al., 2017). However, in the lysogenic life cycle, the phage does not lyse the host cell immediately, but integrates its genome into the host chromosome as a prophage or can also exist as an episomal element such as phage P1 (Yarmolinsky and Sternberg, 1988). This prophage replicates along with the bacterial host genome. Prophage elements can be a major source of new genes and, often, of new functions in bacterial genomes such as pathogenicity islands, toxins, or super infection immunity (Brüssow, 2007; Brüssow et al., 2004). The lysogenic life cycle exists until the prophage is induced, often in response to host stress. Prophages are canonically induced when antibiotic treatment, oxidative stress, or DNA damage activates the bacterial SOS response (Penadés et al., 2015). Upon induction, the prophage excises from the host genome and activates its replication cycle; the expression of phage DNA follows, and the lytic cycle begins (Doss et al., 2017).

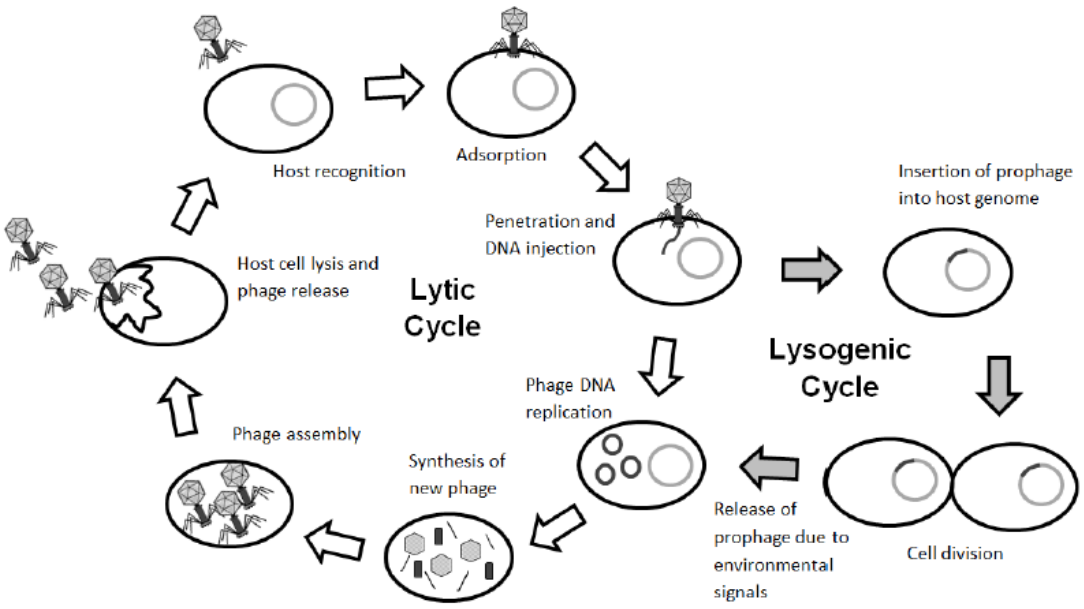

Figure 3. The two life cycles of a phage. White arrows show the lytic life cycle, and the grey arrows show the lysogenic cycle. After infecting the cell, a decision between lytic or lysogenic will be determined by the phage shortly. In the lytic cycle, new phage particles are produced and released upon host cell lysis. In the lysogenic cycle, phage DNA is integrated into host genome or existed as an episomal element, and replicated together with the host chromosome when cell division occurs (Figure adapted from Doss et al., 2017).

Bacteriophages as biocontrol agents

Phages were discovered independently by Frederick Twort in 1915 and Felix d'Herelle in 1917 and were immediately recognized as potential antimicrobial agents (Duckworth, 1976). The capability of phages to kill host cells at the end of the infectious cycle is the cornerstone of the idea of using phages as therapeutic agents (Skurnik and Strauch, 2006). Lytic phages can provide specific, nontoxic antimicrobial action against specific target bacterial pathogens (Koskella and Taylor, 2018). The isolation of phages is fast, relatively simple, and inexpensive (Parasion et al., 2014). Phages can stay infective under harsh environmental conditions and tend to replicate indefinitely, as long as susceptible host bacteria are present (Schmelcher and Loessner, 2014). Phages as

biocontrol agents possess advantages over chemical controls in that tailor-made cocktails of different phages can be adapted to target specific disease-causing bacteria, and to combat bacterial resistance, which may develop over time (Buttimer et al., 2017). Furthermore, the lack of chemical control options and the increases in antibiotic resistance in many plant pathogens combined with consumer preference for organic and antibiotic-free products has led to a phage therapy renaissance in agriculture (Svircev et al., 2018). Over the years, multiple phage-phytopathogen-plant systems have been studied, and promising results are beginning to emerge (Frampton et al., 2012). Thus, bacteriophages offer an effective and sustainable biocontrol system for citrus canker caused by *Xac.*

CHAPTER II

ISOLATION AND CHARACTERIZATIONS OF PHAGES

Introduction

As previously stated, phages are the most numerous and most diverse life forms on earth, therefore environmental samples that include water, plants and soil were directly assayed and/or enriched using *Xac* strains to isolate phages. The objective of the study was to isolate virulent phages for *Xac*, since only virulent and non-transducing should be implemented for the development of an effective and sustainable phage-based control system (Gill and Hyman, 2010). The term virulent simply means that each phage-infected cell generates progeny phage particles and undergoes lysis. In addition, Gill and Hyman (2010) suggested that temperate phages should be avoided when using phage as biocontrol agents to achieve therapeutic purpose (Gill and Hyman, 2010). Critical parameters that affect phage therapy are phage adsorption rate, burst size and latent period (Payne and Jansen, 2001). Latent period, the time between adsorption and cell lysis, determines the speed of replication, while burst size represents average production of virions per infected cell (Abedon, 2009). Larger burst sizes and lower latent periods will produce more virions, which are beneficial in phage treatments (Gill and Hyman, 2010). However, temperate phages may carry harmful genes, thus a full annotation of the phage genome sequence is needed to determine the life style of phage to be used as a biocontrol prevent possible complications during phage therapy (Skurnik and Strauch, 2006).

Materials and methods

Phage isolation

Environmental samples including water, soil, and weeds were collected and processed to isolate phages. Soil samples (10 g) were mixed with 20 ml of 0.125 M phosphate buffer, pH 7.1, amended with 1% peptone (final concentration). This mixture was shaken for 18 h at 28º C, 150 rpm in a 100 ml Erlenmeyer flask, centrifuged at 9,168 x g for 20 min at 5º C and filtered through a 0.22 μm filter. The filtrate (soil extract) was stored at 4º C. For weed samples, 10 g of chopped plant tissue was added in 20 ml of phosphate buffer and processed using a Waring blender. The sample was filtered through double-layered cheese cloth to remove plant tissue, centrifuged at 9,168 x g for 20 min at 5º C and filtered through 0.22 μm filter. The extract was stored at 4º C. Water samples (50 ml of each) were centrifuged, filter sterilized (0.22 μm) and stored as stated above.

Phage enrichments were conducted by adding plant, soil or water filtrates to mid-log broth cultures of *Xac* isolates and incubating the mixtures. Briefly, the bacterial isolates were grown on NBY agar plates (Vidaver, 1967) containing no glucose (MNBY) for 18 h at 28º C. The MNBY broth was inoculated with a suspension of freshly grown *Xac* culture. The broth culture (25 ml) was adjusted to a starting OD_{600} of 0.08, and incubated at 28º C (180 rpm). Five ml of each filtrate (soil, weed, or water) was added to the individually growing cultures along with five ml of 2x MNBY broth at OD_{600} = 0.5 (~5 x 10^8 CFU/ml). After 18 h, the enrichments were centrifuged at 9,000 x g for 20 min at 5°C. The supernatants were filtered through 0.22 μm filter and stored at 4º C.

The enrichment filtrates were evaluated for phage by spot testing. Twenty μl of a dilution series of the filtrates was spotted on the surface of a 0.4% top MNBY agar overlay

supplemented with 1mM $MgSO_4$ (final concentration) that was seeded with 100 µl of suspension of individual *Xac* strains (OD_{600} = 0.5). Plates were incubated inverted overnight in 28º C and observed for the presence of plaques. Samples resulting in plaques were serially diluted and titered using the overlay method. Briefly, 100 µl each of bacterial suspension (OD_{600} = 0.5) and a serial dilution of phage positive enrichments were added to the 5ml of 0.4% top agar and overlayed on a MNBY agar plate. Plaques exhibiting different morphologies were plaque purified three times using single-plaque purification method (Summer et al., 2010). Plaques from the third sub-culture were used to produce high titer phage stock lysates using the method of Lysenko et al. (1974).

Transmission electron microscopy

The phage samples were negatively stained using a modified Valentine method (Valentine et al., 1968). A drop of 50 µl of phage lysate (~ 10^9 - 10^{10} PFU/ml) and 2% uranyl acetate was pipetted onto pre-cut strip of Parafilm. A small piece of carbon–coated mica was dipped into the phage lysate with the carbon film side facing up at a 45 degree angle for one minute and then placed onto the drop of 2% uranyl acetate staining for 10 seconds. A cleaned 300 mesh copper grid was used to pick up the carbon film, and excess stain was removed from the side of the grid. The phage morphology was determined by using a JEOL1200EX TEM at 100 kV accelerating voltage performed at Texas A&M Microscopy and Imaging Center. Images were recorded at calibrated magnifications by the use of a charge-coupled-device (CCD) camera, and measurements acquired using Image J software.

Host range study

A panel of 13 *Xac* and *Xanthomonas* sp. were used to determine the host range of isolated phages. The strains are listed in Table 2. The host(s) used in the phage enrichments were used as the plating control(s) in the study.

Table 2. Host range study test panel.

Strain ID	Genus/species/relevant feature	Origin	Source
EC-12	*Xanthomonas* sp., rice isolate (ATCC PTA-13101)	Texas	(Ahern et al., 2014)
EC-12-1	EC-12; unmarked deletion of *pilA*	Texas	(Ahern et al., 2014)
North 40	*X. axonopodis* pv. citri, sweet orange isolate	Florida	Wang, N.[a]
Ft. Basinger	*X. axonopodis* pv. citri, sweet orange isolate	Florida	Wang, N.
Block 22	*X. axonopodis* pv. citri, sweet orange isolate	Florida	Wang, N.
306	*X. axonopodis* pv. citri, pathotype A	Brazil	Hartung, J.S.[b]
XS2000-00060	*X. axonopodis* pv. citri, pathotype A	Florida	Jones, D.[b]
W-4	*X. axonopodis* pv. citri, Wellington group (A^W)	Florida	Jones, D.
XI2000-00120	*X. axonopodis* pv. citri, Miami group	Florida	Jones, D.
XS1999-00038	*X. axonopodis* pv. citri, Miami group	Florida	Jones, D.
XS2003-00004	*X. axonopodis* pv. citri, Manatee group	Florida	Jones, D.
XN2003-0011-1	*X. axonopodis* pv. citri, Etrog group	Florida	Jones, D.
XN2003-0013-2	*X. axonopodis* pv. citri, Etrog group	Florida	Jones, D.

[a] University of Florida
[b] Florida Department of Agriculture and Consumer Services, Division of Plant Industry, Gainesville, FL

Phage genomic DNA extraction

The phage lysates of plaque purified phage (>10^9 PFU/ml) were treated with DNase and RNase to final concentration of 2 units/ml at 37º C for 30 mins to degrade the host DNA and RNA. Phage particles were precipitated by adding precipitant solution

(10% w/v PEG-8000, 1M NaCl final concentration) to the lysate at a ratio of 1:2 (precipitant: lysate), mixed gently by inversion, and incubated for 18-24 h at 4º C. The mixture was centrifuged at 10,000 x g, 4º C for 10 min and the supernatant was discarded. The pellet was resuspended in 500 µl of 5 mM $MgSO_4$ and transferred to a new labeled 1.5 ml microcentrifuge tube. This sample was centrifuged for 5-10 sec to pellet any insoluble particles and the supernatant transferred to a new 2 ml microcentrifuge tube. One ml of resin from Promega Wizard Kit (Cat. No: A7280) was added to the phage suspension and mixed by inverting the tube 5-6 times. The DNA extraction was performed using the protocol provided with the kit. Phage DNA was stored at -20 ºC.

Phage genome sequencing and annotation

Phage DNA was sequenced using the Illumina MiSeq platform to generate paired-end 250 bp reads according to manufacturer's guidelines. FastQC (bioinformatics.babraham.ac.uk), FastX Toolkit (hannonlab.cshl.edu), and SPAdes 3.5.0 (Bankevich et al., 2012) were used for read quality control, read trimming, and read assembly, respectively. The completed contig was confirmed via PCR off the genome ends with phage specific primer sets (Table 3). The product of PCR amplification was sequenced by Sanger sequencing (Eton Bioscience, San Diego, CA). The contig sequence was manually corrected to match the resulting Sanger sequencing reads. Genes were predicted using Glimmer3 (Delcher et al., 1999) and MetaGeneAnnotator (Noguchi et al., 2008); and their functions were assigned using InterProScan (Jones et al., 2014), BLAST (Camacho et al., 2009) and other tools available in the Web Apollo instance (Lee et al., 2013) hosted by the Center for Phage Technology (CPT) (https://cpt.tamu.edu/galaxy), and all analyses were performed in the Galaxy interface (Afgan et al., 2018).

Table 3. Primers used in Chapter II for closing the assembled genomes.

Primer	Sequence	Reference
CCP504-End-F	5'-ACCTATAGCACACAGTGCCG-3'	This study
CCP504-Beg-R	5'-GGCTTCCCGTTACACCCTAC-3'	This study
CCP513-End-F	5'-GGGACCCGGACAACGAATAC-3'	This study
CCP513-Beg-R	5'-CGCCGAAGTTGTCCAGGTTG-3'	This study
CCP509-End-F	5'-GTGCAATCCTGACACCGCTG-3'	This study
CCP509-Beg-R	5'-CACGCGCCGTGACATAACTC-3'	This study

Adsorption assay

Liquid culture of logarithmically growing cells (OD_{600} ~ 0.5) was mixed with individual phage at an MOI ~ 0.1. The mixture was incubated at 28 ºC with shaking (~150 rpm). Samples of unabsorbed phages were taken at 3 min intervals and immediately filter sterilized. The supernatant were serial diluted and plated for plaque count. The rate of phage adsorption is defined as $dP/dt = -kBP$, where k is adsorption constant in ml $cell^{-1}$ min^{-1} , B is the bacteria concentration, and P is the free phage concentration at time of interest (Schwartz, 1975).

One-step growth curve

The one step growth curve is the standard method used in defining the latent period and the average burst size for phage characterization (Delbrück, 1945). Liquid culture of logarithmically growing cells (OD_{600} = 0.5) was mixed with individual phage at an MOI of ~ 0.1 at 28º C for 5 minutes. After 5 min of adsorption, the phage mixture was diluted 1000-fold to stop further adsorption (defined as flask A). Flask A was then diluted another 100-fold (defined as flask B). Both flasks were incubated immediately at 28º C with constant shaking (150 rpm). Samples were taken at 3-min intervals and plated for plaque counts. The counts should remain constant until a sudden increase, which points to cell

lysis. The period between initial adsorption and the sudden increase was defined as latent period. The plaque count at cell lysis divided by adsorbed phage count was defined as burst size.

Microtiter plate assay

A single colony in overnight broth culture of *Xac* (strain Block 22) was diluted and adjusted to OD_{600} = 1.0 (~ 10^9 CFU/ml) spectrophotometrically with MNBY broth, then used as inoculum for loading into Falcon 96 well flat bottom plate (Corning, Cat. No. 351172). Phage lysates were tittered and adjusted with P-buffer (50 mM Tris-HCl pH 7.5, 100 mM NaCl, 8 mM MgSO4) to the desire concentation of 10^7, 10^8, 10^9 PFU/ml prior loading on the plate. For each well, 160 µl of MNYB broth was added along with 20 µl of *Xac* (~ 10^8 CFU/ ml final concertation) and 20 µl of phage (~ 10^6, $10^7$and 10^8 PFU/ml final concentration) to achieve multiplicity of infection (MOI) of 0.1, 1 and 10, respectively. The plate was incubated at 28º C with double orbital shaking at 150 rpm in a Tecan Spark 10 M plate reader (Tecan Group Ltd., Männedorf, Switzerland). The growth was monitored at 30 min intervals for 20 h by measuring OD_{600}. After baseline adjustment, growth curves were generated by plotting OD_{600} measurements against time. All assays were done in triplicate.

Results and discussion

Phages isolation and characterization

Thirty nine phages were isolated from enriched sewage water and plant filtrates using *Xanthomonas* EC-12 or *Xac* sweet orange isolates as the host. The phages were then divided into six groups based on their host range as determined using the panel described

in Table 2. Three phages with different morphologies and host range groups were chosen for further characterization. The phages were designated CCP504, CCP513, and CCP509.

Phage CCP504 was isolated from a water sample collected at Wolf Pen Creek in College Station, Texas, using *Xac* strain Ft. Basinger as host for enrichment. Phages CCP505 and CCP511 were isolated from water samples collected at Lick Creek and Cater Creek waste water treatment plants located in College Station and Bryan, Texas, respectively, using EC-12 as host for enrichment. Phages CCP513 and CCP509 isolated from sewage water samples collected from the Carter Creek and Lick Creek waste water treatment plants located in Bryan and College Station, Texas, respectively, using *Xac* strain Block 22 as the host for enrichment.

The host range and physical properties of the three selected phages are summarized in Table 4, 5 and Figure 4. Phage CCP504 exhibited podophage morphology with an isometric head of 50 nm in diameter and a short stubby non-contractile tail (Figure 4a, Table 5). Phage CCP513 exhibited siphophage morphology with an isometric head of 57 nm in diameter and a long non-contractile tail of 122 nm in length (Figure 4b, Table 5). Phage CCP509 exhibited myophage morphology with an isometric head of 97 nm in diameter and a long contractile tail of 149 nm in length (Figure 4c, Table 4). All three selected phages formed plaques on *Xanthomonas* spp. and/or *Xac* strains with differences in their host range (Table 4). The podophage formed large, clear plaques, whereas the siphophage and myophage formed small, clear plaques.

Full characterization was conducted on selected phages CCP504, CCP513 and CCP509. However, podophages CCP504, CCP505 and CCP511 and siphophage CCP513 were used as a cocktail to determine the efficacy of the phages to control citrus canker in

greenhouse studies (See Chapter IV). The four phages were chosen based on host range differences (Table 4), morphology and preliminary annotation of sequenced genomes (data not shown).

Table 4. Phages host range.

Strain ID	**Phage designation and host range**				
	CCP504	**CCP505**	**CCP511**	**CCP513**	**CCP509**
EC-12	+[a]	+	+	-	+
EC-12-1	-	-	-	-	-
North 40	+	+	+	+	+
Ft. Basinger	+	+	+	+	+
Block 22	+	+	+	+	+
306	-	-	-	-	-
XS2000-00060	-	-	-	-	-
W-4	+	-	-	+	+
XI2000-00120	+	+	+	+	+
XS1999-00038	+	+	+	+	+
XS2003-00004	-	-	-	-	-
XN2003-0011-1	-	-	+	-	+
XN2003-0013-2	-	-	+	-	+

[a] Ability to form individual plaques on indicated host

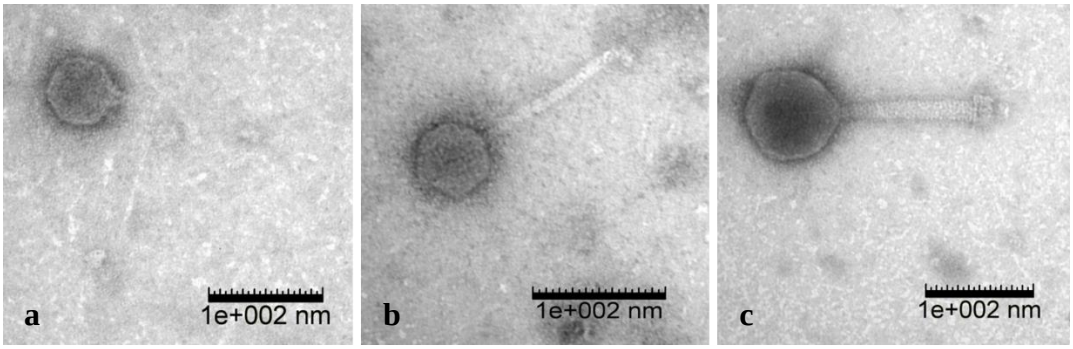

Figure 4. Phage TEM image of selected phages. (a) CCP504, (b) CCP513, (c) CCP509. Samples were negatively stained with 2% (wt/vol) aqueous uranyl acetate. Additional information is shown in Table 5.

Table 5. General, physiological, and structural characteristics of *Xac* phages.

	CCP504	**CCP513**	**CCP509**
Morphology	Podo	Sipho	Myo
Capsid width (nm)	50	57	97
Tail length (nm)	-	122	149
Mean k (ml $cell^{-1}$ min^{-1})	1.52 x 10^{-10}	1.12 x10^{-10}	2.01 x 10^{-10}
Latent period (min)	30	30	21
Mean burst size (PFU $cell^{-1}$)	50	75	48
Genome size (kb)	44.5	42.5	199

[a] k = adsorption constant

Adsorption constants were determined from three replicate experiments using strain Block 22 as host. The observed adsorption constants for the three phages were 1.52 x 10^{-10}, 1.21 x 10^{-10} and 2.01 x 10^{-10} ml $cell^{-1}$ $min^{-1,}$ for CCP504, CCP513 and CCP509, respectively. An average burst size of three phages were between 50-75 PFU $cell^{-1}$ at approximately 30 min for CCP504 and CCP513 and 21 min for CPP509 (Table 5).

Liquid infection assays

The efficacy of CCP504, CCP513, and CCP509 against *Xac* strain Block 22 in liquid culture were assessed at MOIs of 0.1, 1 and 10 within a time frame of 20 h (Figure 5). The result of this assay showed significant suppression of *Xac* Block 22, when phages were added compared to the bacterial control at all tested MOI. However, phage CCP504 showed little variation in the growth suppression of Block 22 (Figure 5a). In contrast, CCP513 and CCP509 are dependent on the MOI used, as MOI increased, the growth of the culture significantly decreased (Figure 5b and c).

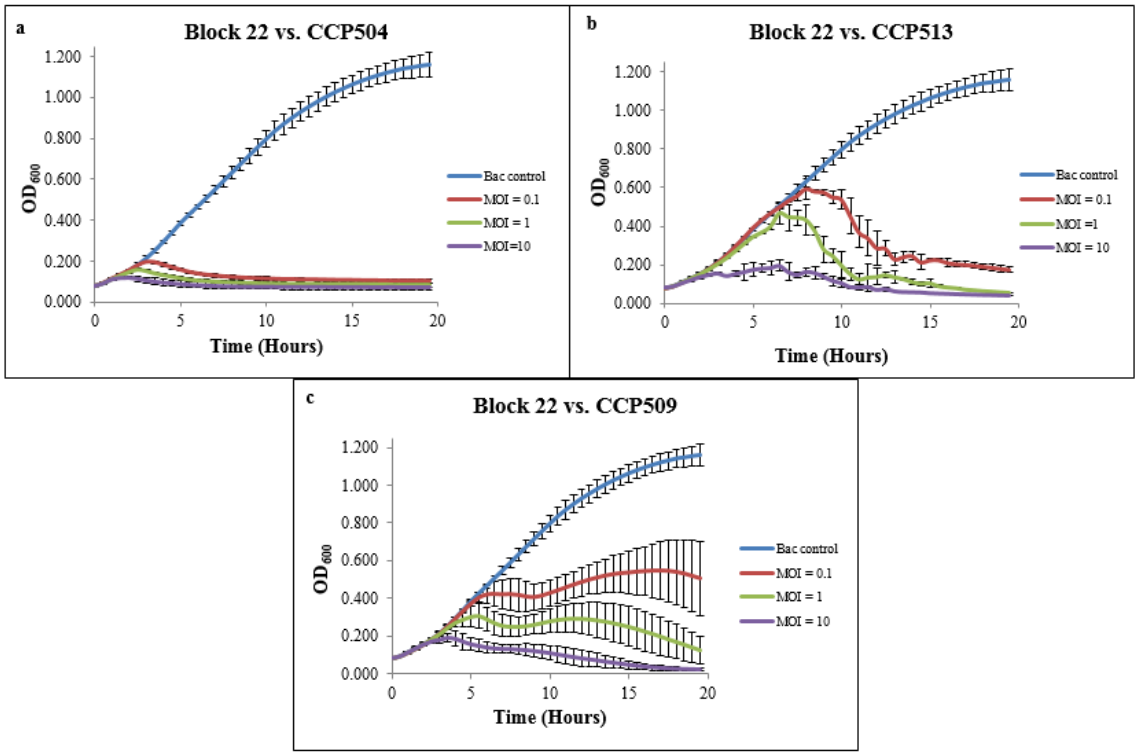

Figure 5. Phage ability to kill *Xac* strain Block 22 cells in liquid culture at different MOIs (a) Block 22 vs. CCP504 (b) Block 22 vs. CCP513 (c) Block 22 vs. CCP513. The experiments were performed in triplicate, bars indicate standard deviation.

Phage genomes analysis

Phage CCP504

CCP504 is a podophage with a 44,551 bp genome, a coding density of 96.4% and a G+C content of 62.4%. Genome annotation revealed 59 protein coding sequences, of which 26 have a predicted function as determined by BLASTp and InterProScan. Using PhageTerm (Garneau et al., 2017), a nonpermutated direct terminal repeat of 405 bp was predicted. CCP504 shared 79.97, 77.92, and 71.84% nucleotide sequence identity with *Xanthomonas* phage f30-Xaj (KU595433.1), *Xanthomonas* phage f20-Xaj (KU595432.1), and *Xylella* phage Prado (KF626667.1), respectively, as determined by Mauve alignment

(Darling et al., 2004). CCP504 is phiKMV-like based on the genomic orientation and protein homology range from 36 to 86% with other phiKMV-like phages (Ahern et al., 2014; de Leeuw et al., 2017; Lavigne et al., 2003). Similar to other phiKMV-like phages, phage CCP504 contains a single subunit RNA polymerase (RNAP) at the end of class II gene cluster of DNA metabolism. CCP504 metabolism genes follow the order of phiKMV-like phages: DNA primase, DNA helicase, DNA polymerase, ribonuclease H-like superfamily, DNA ligase, and RNAP. In the lysis cassette of CCP504 the holin gene is found upstream of the endolysin, separated by terminase small subunit, terminase large subunit and a hypothetical protein, respectively. The holin gene belongs to class III holin consist with a single transmembrane domain (TMD). The endolysin showed characteristic of a SAR endolysin that exhibits an N-terminal hydrophobic domain rich in weakly hydrophobic residues (Xu et al., 2004b). A Glycoside hydrolase, family 24 (IPR002196) is predicted by InterProScan and contains an E-8 aa-D-5 aa-T catalytic triad, a characteristic of true lysozymes found in T4 protein E (Kuty et al., 2010). CCP504 also encodes the two component spanins, which has the o-spanin partially embedded in the i-spanin, resulted in the disruption of the outer membrane in Gram negative host.

The genomes of two other podophages (CCP505 and CCP511) were also partially annotated (data not shown). Both phages were determined to be phiKMV-like phages, since both they encode a single-subunit RNA polymerase (RNAP) at the end of the class II gene cluster rather than in the early genomic region (Lavigne et al., 2003). Although not fully annotated the two phages were used in greenhouse efficacy studies (See Section IV).

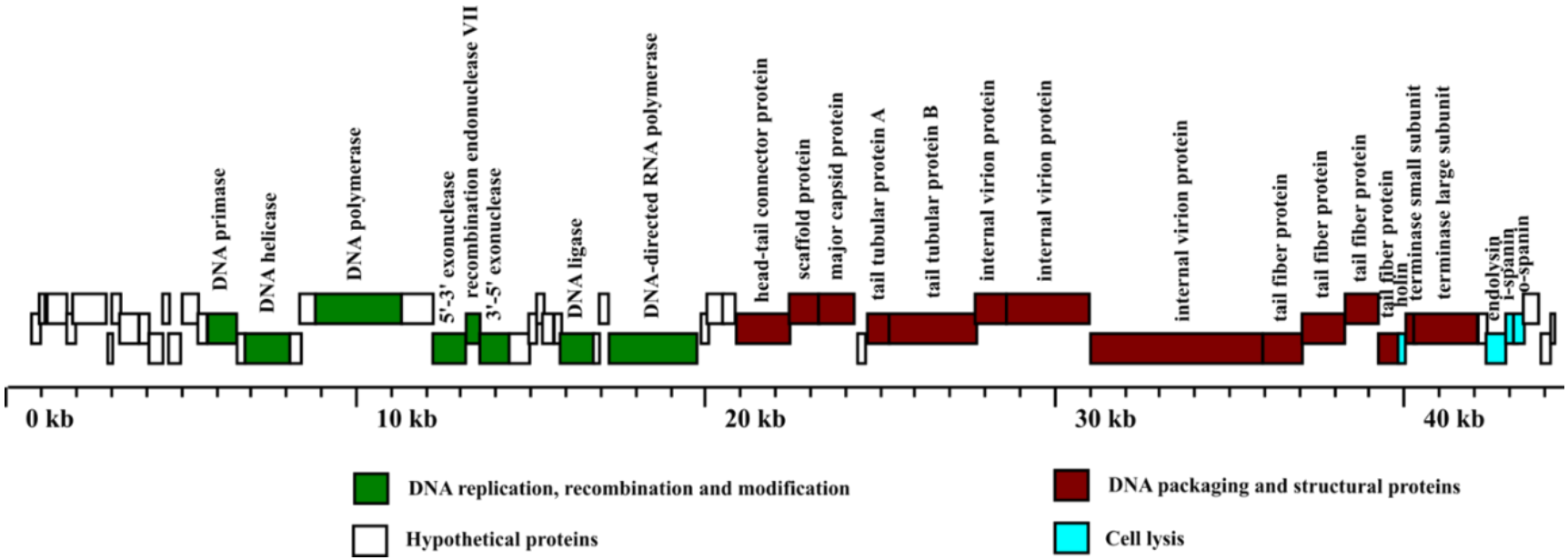

Figure 6. CCP504 genome map.

Table 6. CCP504 putative genes and homologues.

GP[a]	Name	Start	End	Strand	Length (AA[b])	Representative homologue	E value
gp1	Hypothetical protein	704	966	+	84		
gp2	Hypothetical protein	949	1109	+	49		
gp3	Hypothetical protein	1132	1699	+	186	A0A249XLE5_9CAUD Uncharacterized protein OS=*Xanthomonas* phage phi Xc10	1.70E-117
gp4	Hypothetical protein	1685	1944	+	82		
gp5	Hypothetical protein	1894	2857	+	317		
gp6	Hypothetical protein	2907	3048	+	42		
gp7	Hypothetical protein	3001	3262	+	82		
gp8	Hypothetical protein	3242	3794	+	180		
gp9	Hypothetical protein	3776	4065	+	93		
gp10	Hypothetical protein	4053	4457	+	130		
gp11	Hypothetical protein	4444	4642	+	63		
gp12	Hypothetical protein	4629	4977	+	113		
gp13	Hypothetical protein	5038	5505	+	151		
gp14	Hypothetical protein	5489	5753	+	84		
gp15	DNA primase	5759	6590	+	274	V5Q8P0_9CAUD DNA primase	6.66E-170
gp16	Hypothetical protein	6573	6817	+	77		
gp17	DNA Helicase	6795	8093	+	429	IPR027417	2.90E-04
gp18	Hypothetical protein	8079	8407	+	106		
gp19	Hypothetical protein	8389	8850	+	149		
gp20	DNA Polymerase	8836	11312	+	822	NP_041982.1 T7_gene_5 DNA polymerase A , IPR001098	5.43E-10
gp21	Hypothetical protein	11311	12220	+	298		
gp22	5'-3' Exonuclease	12207	13149	+	310	IPR020045	5.53E-11
gp23	Recombination endonuclease VII	13130	13532	+	129	IPR00421	3.70E-13

Table 6. Continued

GP	Name	Start	End	Strand	Length (AA)	Representative homologue	E value
gp24	3'-5' exonuclease	13518	14356	+	276	IPR012337	2.23E-16
gp25	hypothetical protein	14355	14944	+	193		
gp26	hypothetical protein	14915	15143	+	71		
gp27	hypothetical protein	15133	15352	+	70		
gp28	hypothetical protein	15341	15661	+	103		
gp29	hypothetical protein	15638	15854	+	67		
gp30	DNA ligase	15837	16813	+	321	DNLI_NATPD DNA ligase	3.57E-04
gp31	hypothetical protein	16797	16977	+	56		
gp32	hypothetical protein	16966	17231	+	85		
gp33	DNA-directed RNA polymerase	17223	19743	+	837	NP_041960.1 T7_gene_1 RNA polymerase , IPR002092	4.81E-106
gp34	hypothetical protein	19850	20070	+	70		
gp35	hypothetical protein	20020	20506	+	157		
gp36	hypothetical protein	20497	20857	+	116		
gp37	head-tail connector protein	20855	22397	+	511	NP_041995.1 T7_gene_8 head-tail connector protein , IPR020991	1.88E-48
gp38	scaffold protein	22378	23245	+	284	V5Q8R0_9CAUD Scaffold protein	6.47E-101
gp39	major capsid protein	23251	24272	+	335	NP_041998.1 T7_gene_10A major capsid protein,	4.04E-04
gp40	hypothetical protein	24336	24564	+	72		
gp41	tail tubular protein A	24611	25239	+	206	NP_041999.1 T7_gene_11 tail tubular protein A, IPR033767	3.82E-11
gp42	tail tubular protein B	25238	27753	+	835	NP_042000.1 T7_gene_12 tail tubular protein B	2.25E-12
gp43	putative internal virion protein	27739	28637	+	295	V5Q8R5_9CAUD Internal virion protein	8.63E-154
gp44	putative internal virion protein	28621	30994	+	786	V5Q7R6_9CAUD Internal virion protein	0

Table 6. Continued

GP	Name	Start	End	Strand	Length (AA)	Representative homologue	E value
gp45	putative internal virion protein	30993	35916	+	1637	IPR023346	1.10E-13
gp46	tail fiber protein	35964	37096	+	374	IPR005604	1.90E-07
gp47	tail fiber protein	37088	38310	+	404	V5Q9R3_9CAUD Tail fiber protein	0
gp48	tail fiber protein	38296	39251	+	315	V5Q8S0_9CAUD Tail fiber protein	0
gp49	tail fiber protein	39231	39829	+	194	V5Q7S0_9CAUD Tail fiber protein	8.73E-137
gp50	holin	39834	40046	+	67	V5Q7X0_9CAUD Holin OS=*Xylella* phage Prado	8.83E-33
gp51	terminase small subunit	40016	40317	+	97	V5Q7T5_9CAUD Terminase small subunit	4.44E-35
gp52	terminase large subunit	40292	42118	+	603	NP_042010.1 T7_gene_19 terminase large subunit	7.22E-81
gp53	hypothetical protein	42110	42368	+	83		
gp54	endolysin	42357	42923	+	184	ENLYS_BPKMV SAR Endolysin OS=*Pseudomonas* phage phiKMV, IPR002196	2.31E-17
gp55	i-Spanin	42887	43222	+	107	V5Q7X5_9CAUD i-spanin	2.94E-04
gp56	o-Spanin	43109	43421	+	100	V5Q7T9_9CAUD o-spanin	2.13E-13
gp57	hypothetical protein	43408	43849	+	144	IPR029055	3.09E-07
gp58	hypothetical protein	43881	44157	+	92		
gp59	hypothetical protein	44186	44306	+	37		

[a] GP = Gene products
[b] AA = amino acid

Phage CCP513

CCP513 is a siphophage with a 42,598 bp genome, a coding density of 94.6% and a G+C content of 62.6%. Genome annotation revealed 56 protein coding sequences, of which 33 have a predicted function as determined by BLASTp and InterProScan and no predicted tRNAs. Using PhageTerm (Garneau et al., 2017), a headful packaging was predicted. Progressive MAUVE algorithm (Darling et al., 2004) showed approximately 19% DNA sequence similarity to others *Pseudomonas phages* in the NCBI nucleotide database including vB_PaeS_PAO1_Ab18 (LN610577.1), vB_PaeS_PAO1_Ab20 (LN610585.1), PaMx11 (JQ067087.2) and AAT-1 (KU204984.2). At protein level, CCP513 shared 28, 29, and 30 unique proteins with Vibrio phage VpKK5 (KM378617.2), *Pseudomonas* phage NP1 (KX129925.1) and *Pseudomonas phage* PaMx25 (JQ067084.3), respectively. Genes related to DNA morphogenesis and metabolism were identified. Unlike CCP504 and CCP509, the lysis cassette of CCP513 includes the endolysin (D-alanyl-D-alanine carboxypeptidases), holin and two component spanins identified in a cluster. The holin gene belonged to class I holin consist with three TMDs with N-out, C-in topology. The o-spanin gene is partially embedded in the i-spanin gene. Tail assembly chaperone with a frameshifted protein product is followed by the tape measure protein analogous to the well-studied lambda G/GT chaperone system (Xu et al., 2004a).

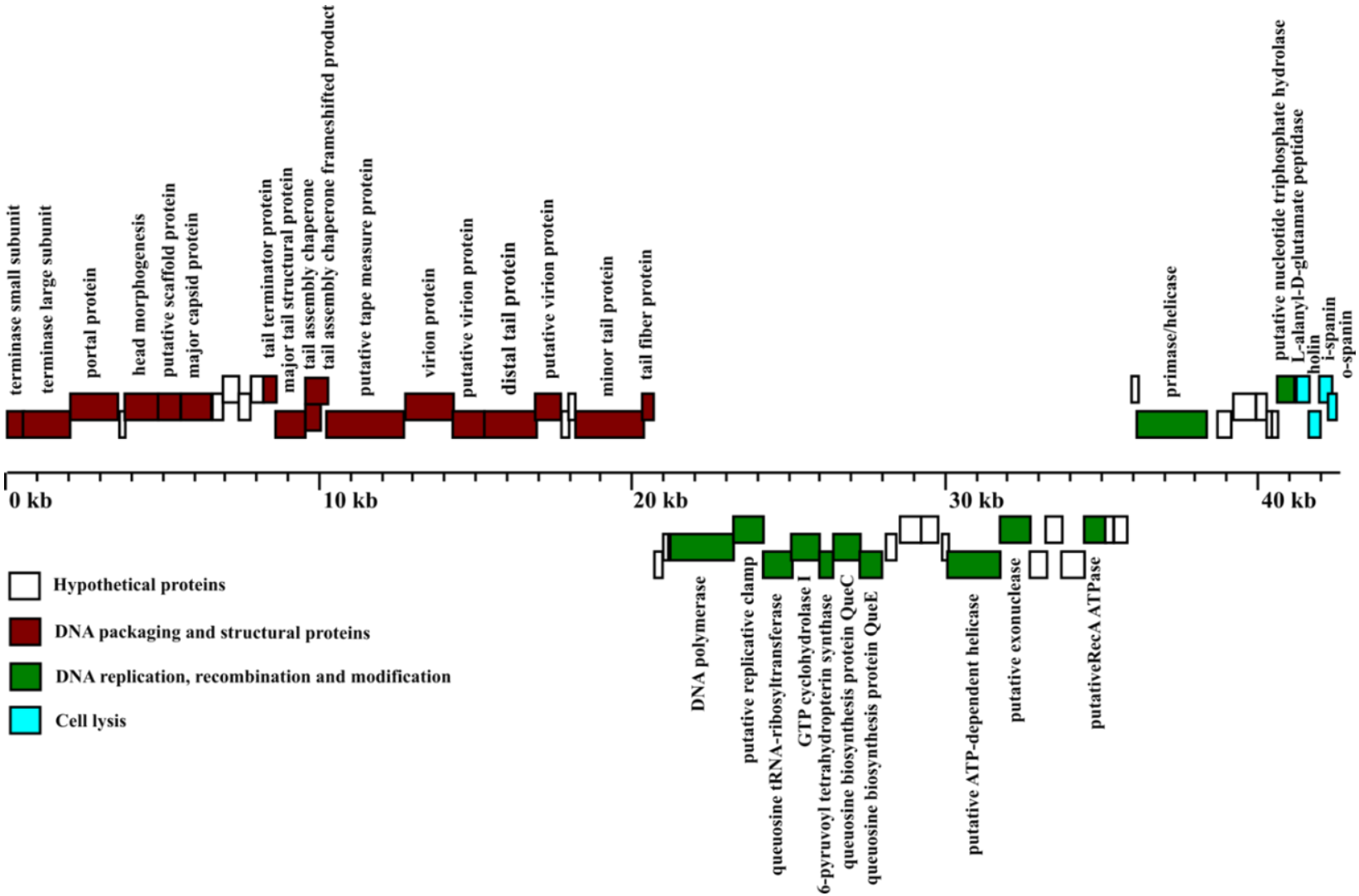

Figure 7. CCP513 genome map.

Table 7. CCP513 putative genes and homologues.

GP[a]	Name	Start	End	Strand	Length (AA[b])	Representative homologue	E value
gp1	terminase small subunit	3	542	+	176	IPR005335	1.20E-07
gp2	terminase large subunit	528	2034	+	502	A0A1X9IAM3_9CAUD Terminase large subunit OS=*Xanthomonas* phage Xoo-sp2	
gp3	portal protein	2033	3553	+	503	H6WTZ6_9CAUD Portal protein OS=*Pseudomonas* phage vB_Pae-Kakheti25 , IPR025129	5.21E-173
gp4	hypothetical protein	3606	3794	+	57		
gp5	head morphogenesis	3770	4848	+	355	IPR006528,	8.90E-10
gp6	putative scaffold protein	4877	5600	+	241	A0A0M3MWV9_9CAUD Scaffold protein OS=*Stenotrophomonas* phage vB_SmaS-DLP_2	2.37E-46
gp7	major capsid protein	5588	6562	+	320	A0A0M3WLU8_9CAUD Major capsid protein OS=*Stenotrophomonas* phage vB_SmaS-DLP_2	7.00E-142
gp8	hypothetical protein	6605	6944	+	109		
gp9	hypothetical protein	6943	7456	+	167	I6NRE5_9CAUD Uncharacterized protein OS=*Burkholderia* phage KL1	4.13E-33
gp10	hypothetical protein	7439	7809	+	119		
gp11	hypothetical protein	7795	8204	+	133	YP_003902.1 T1_gp43 hypothetical protein	1.99E-09
gp12	tail terminator protein	8188	8608	+	136	A0A0S0MVB0_9CAUD Tail terminator protein OS=*Pseudomonas* phage PaMx28 , IPR025395	6.56E-35
gp13	major tail structural protein	8610	9562	+	313	A0A0S0N828_9CAUD Major tail structural protein OS=*Pseudomonas* phage PaMx11	4.39E-170
gp14	tail assembly chaperone	9548	10038	+	308	IPR014859	1.40E-05
gp15	tail assembly chaperone frameshift product	10007	10280	+	91		
gp16	putative tape measure protein	10254	12729	+	822	TMP_BPPAJ Probable tape measure protein OS=*Pseudomonas* phage PAJU2	2.28E-07

Table 7. Continued

GP	Name	Start	End	Strand	Length (AA)	Representative homologue	E value
gp17	virion structural protein	12728	14268	+	510	A0A0S0N8F3_9CAUD Virion structural protein OS=*Pseudomonas* phage PaMx25, IPR008979	0
gp18	putative virion protein	14268	15281	+	334	A0A0S0MWN7_9CAUD Putative virion structural protein OS=*Pseudomonas* phage PaMx74	1.21E-158
gp19	distal tail protein	15270	16944	+	554	YP_009101121.1, *Salmonella* phage Chi	2.10E-23
gp20	putative virion protein	16928	17750	+	270	A0A0S0ND36_9CAUD Putative virion structural protein OS=*Pseudomonas* phage PaMx11, IPR019228	9.31E-165
gp21	hypothetical protein	17748	17993	+	78	YP_009101121.1, *Salmonella* phage Chi	1.88E-05
gp22	hypothetical protein	17978	18196	+	69	A0A2H4GXX9_9CAUD Uncharacterized protein OS=*Pseudomonas* phage JG012	1.51E-26
gp23	minor tail protein	18168	20351	+	724	YP_009101121.1, *Salmonella* phage Chi, IPR032876	1.46E-111
gp24	tail fiber protein	20339	20707	+	119	YP_009101121.1, *Salmonella* phage Chi,IPR021251	5.76E-19
gp25	hypothetical protein	20735	20993	-	82	A0A0M3MYX9_9CAUD Uncharacterized protein OS=*Stenotrophomonas* phage vB_SmaS-DLP_2	2.66E-05
gp26	hypothetical protein	20992	21158	-	51		
gp27	DNA polymerase	21229	23254	-	671	IPR001098	2.70E-62
gp28	putative replicative clamp	23238	24201	-	317	A0A0S0N5L1_9CAUD Putative replicative clamp OS=*Pseudomonas* phage PaMx25	1.08E-128
gp29	queuosine tRNA-ribosyltransferase	24188	25124	-	307	Queuosine tRNA-ribosyltransferase OS=*Vibrio* phage VpKK5	1.38E-110
gp30	GTP cyclohydrolase I	25108	26015	-	298	IPR020602	1.80E-69
gp31	6-pyruvoyl tetrahydropterin synthase	26006	26447	-	143	IPR007115	2.80E-28
gp32	queuosine biosynthesis protein QueC	26437	27303	-	284	IPR018317	1.30E-52
gp33	queuosine biosynthesis protein QueE	27296	28010	-	234	A0A0E3M1C4_9CAUD Queuosine Biosynthesis QueE Radical SAM OS=*Enterobacteria* phage JenK1, IPR007197	4.24E-65

Table7. Continued

GP	Name	Start	End	Strand	Length (AA)	Representative homologue	E value
gp34	hypothetical protein	28117	28447	-	106	A0A2I7R531_9VIRU Uncharacterized protein OS=*Vibrio* phage 1.117.O._10N.261.45.E9	1.02E-28
gp35	hypothetical protein	28536	29228	-	227	A5A3S9_9CAUD BcepGomrgp40, *Burkholderia* phage BcepGomr	1.21E-04
gp36	hypothetical protein	29229	29775	-	178	A0A088FAK6_9CAUD Uncharacterized protein OS=*Vibrio* phage VpKK5	5.14E-15
gp37	hypothetical protein	29917	30132	-	67		
gp38	putative ATP-dependent helicase	30077	31769	-	559	YP_003923.1 T1_gp22 putative ATP-dependent helicase, IPR006935, IPR001650	3.07E-16
gp39	putative exonuclease	31755	32728	-	320	A0A172PZV2_9CAUD Putative exonuclease OS=*Pseudomonas* phage NP1, IPR011604	7.32E-117
gp40	hypothetical protein	32714	33264	-	179		
gp41	hypothetical protein	33216	33750	-	173	IPR021686	4.40E-37
gp42	hypothetical protein	33713	34456	-	243	IPR007731	9.80E-18
gp43	putative RecA ATPase	34443	35141	-	228	A0A0S0N5J7_9CAUD Putative RecA ATPase OS=*Pseudomona*s phage PaMx25, IPR027417	1.88E-113
gp44	hypothetical protein	35127	35393	-	85		
gp45	hypothetical protein	35385	35808	-	137	A0A0S0N8R3_9CAUD Uncharacterized protein OS=*Pseudomonas* phage PaMx25 GN=PaMx25_56	8.11E-31
gp46	hypothetical protein	35938	36163	+	70	A0A088F6R6_9CAUD Uncharacterized protein OS=*Vibrio* phage VpKK5	1.19E-06
gp47	primase/helicase	36153	38388	+	741	A0A088FAP0_9CAUD Primase/helicase OS=*Vibrio* phage VpKK5	1.89E-180
gp48	hypothetical protein	38700	39141	+	143	A0A088F6R6_9CAUD Uncharacterized protein OS=*Vibrio* phage VpKK5	4.37E-27
gp49	hypothetical protein	39188	39906	+	236	IPR024498	2.40E-14
gp50	hypothetical protein	39932	40268	+	108	A0A172Q030_9CAUD Uncharacterized protein OS=*Pseudomonas* phage NP1	3.79E-24
gp51	hypothetical protein	40251	40435	+	57		

Table 7. Continued

GP	Name	Start	End	Strand	Length (AA)	Representative homologue	E value
gp52	hypothetical protein	40419	40617	+	61	A0A172PZW8_9CAUD Uncharacterized protein OS=*Pseudomonas* phage NP1	2.49E-09
gp53	putative nucleotide triphosphate hydrolase	40588	41141	+	180	A0A0S0N575_9CAUD Putative nucleotide triphosphate hydrolase OS=*Pseudomonas* phage PaMx28, IPR027417	2.23E-65
gp54	L-alanyl-D-glutamate peptidase	41200	41617	+	135	ENLYS_BPT5 L-alanyl-D-glutamate peptidase OS=*Escherichia* phage T5	1.01E-15
gp55	holin	41607	41983	+	121	YP_001542615.1 Enterobacteria phage PRD1, IPR032126	4.97E-11
gp56	i-spanin	41938	42353	+	134		
gp57	o-spanin	42257	42531	+	88		

[a] GP = Gene products
[b] AA = amino acid

Phage CCP509

CCP509 is a myophage with a 199,186 bp genome, a coding density of 91% and a G+C content of 50.2%. Genome annotation revealed 328 protein coding sequences, of which 87 have a predicted function as determined by BLASTp and InterProScan, and 41 tRNAs were identified with ARAGORN 2.36 (Laslett and Canback, 2004) . Using PhageTerm (Garneau et al., 2017), a headful packaging was predicted. Progressive MAUVE algorithm (Darling et al., 2004) showed little recognizable DNA sequence similarity to other phages in NCBI nucleotide database, less than 7%. However, at protein level, CCP 509 shared 87 and 74 unique proteins with *Stenotrophomonas* phage IME-SM1 (KR560069.1) and *Acidovorax* phage ACP17 (KY979132.2), respectively. CCP509 is a T4-like phage with 45 proteins that are homologous with phage T4 as resulted by BLASTp with E value $\leq 10^{-5}$. Majority of morphogenesis, DNA replication and repair genes of CCP509 were identified. Genes for biosynthesis proteins were also found such as ribonucleoside-diphosphate reductase alpha and beta, deoxynucleoside monophosphate kinase and NAD/GMP synthase, and queuosine biosynthesis QueE radical SAM etc. And similar to T4, the lysis cassette does not cluster together. A glycoside hydrolase type of endolysin (IPR023346) was found upstream from the spanin complex in the 75-80 kb range. The spanins complex contains o-spanin embedded in the i-spanin. However, we were not able identify the location of the holin gene in the genome because there are several genes with TMHMM prediction utilizing for holin classification but did not have predicted gene function based on the BLASTp results.

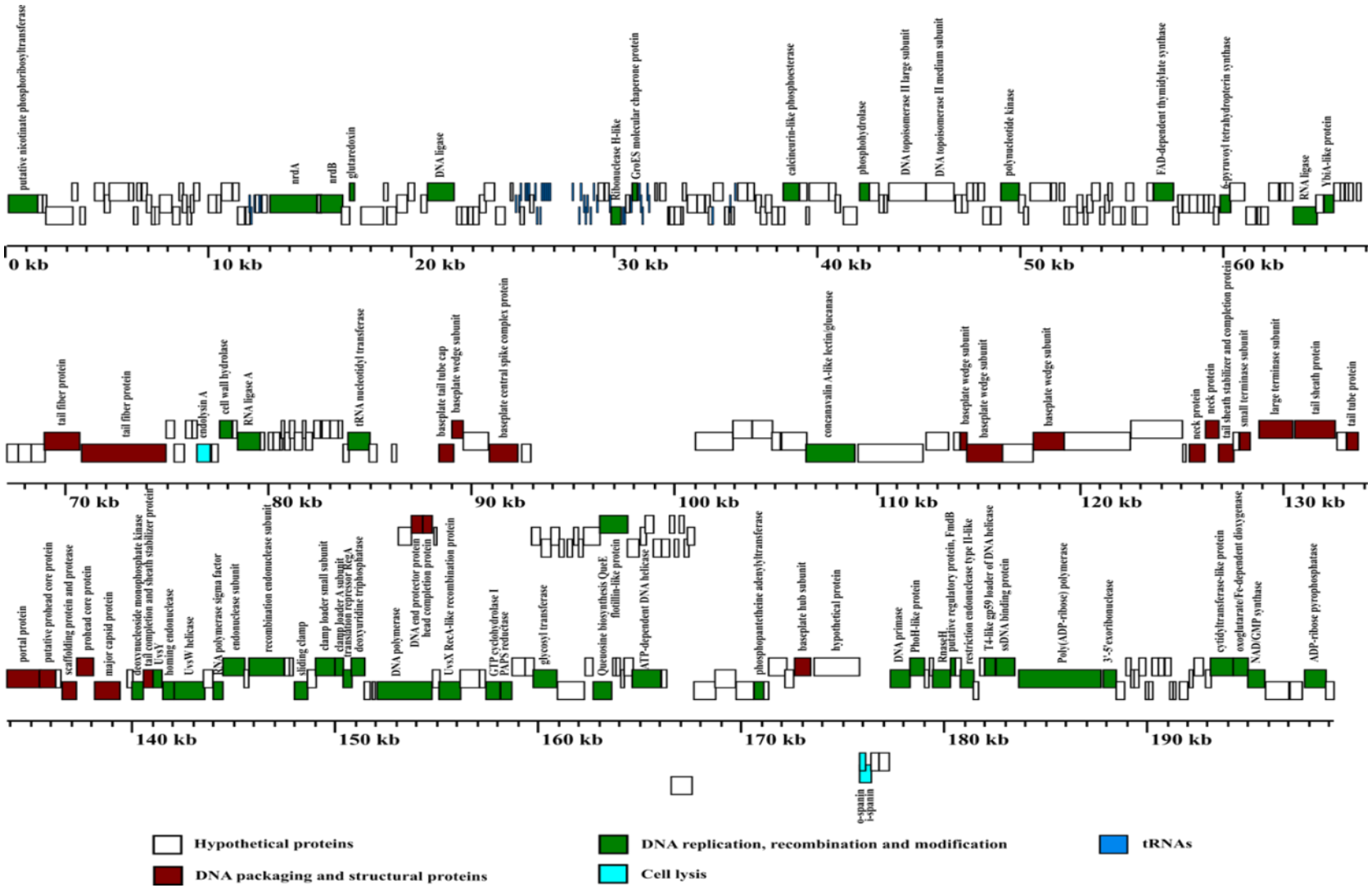

Figure 8. CCP509 genome map.

Table 8. CCP509 putative genes and homologues, and tRNAs predictions.

GP[a]	Name	Start	End	Strand	Length (AA[b])	Representative homologue	E value
gp1	putative nicotinate phosphoribosyltransferase	98	1552	+	481	YP_009041424.1 K_gp064 putative nicotinate phosphoribosyltransferase, IPR007229	3.20E-64
gp2	hypothetical protein	1577	1809	+	74		
gp3	hypothetical protein	1775	1972	+	62		
gp4	hypothetical protein	1959	3288	+	439	A0A1Y5SJ14_9RHOB Uncharacterized protein OS=*Pseudooctadecabacter jejudonensis*	1.64E-18
gp5	hypothetical protein	3271	3553	+	91		
gp6	hypothetical protein	3606	3858	+	84		
gp7	hypothetical protein	4342	4804	+	154	A0A292GDH9_9VIRU Uncharacterized protein OS=*Xanthomonas* phage XacN1	3.26E-30
gp8	hypothetical protein	4847	5131	+	91	Q8SD46_BPDPK PHIKZ116 OS=*Pseudomonas* phage phiKZ	4.23E-11
gp9	hypothetical protein	5119	6081	+	317	A0A0H4ISK8_9CAUD Uncharacterized protein OS=*Stenotrophomonas* phage IME-SM1	2.73E-134
gp10	hypothetical protein	6058	6295	+	75		
gp11	hypothetical protein	6282	6486	+	64		
gp12	hypothetical protein	6478	6694	+	69		
gp13	hypothetical protein	6676	6945	+	85	A0A1B4XX76_9VIRU Uncharacterized protein OS=*Tenacibaculum* phage pT24	5.41E-12
gp14	hypothetical protein	6929	7172	+	77	A0A258ANU9_9BACT Uncharacterized protein OS=*Verrucomicrobia* bacterium 12-59-8	3.03E-07
gp15	hypothetical protein	7158	7351	+	60		
gp16	hypothetical protein	7338	7569	+	73		
gp17	hypothetical protein	7571	8175	+	198	YFDR_ECOLI Uncharacterized protein YfdR OS=*Escherichia coli* (strain K12)	1.33E-37
gp18	hypothetical protein	8199	8553	+	115	A0A0H4ISN2_9CAUD Uncharacterized protein OS=*Stenotrophomonas* phage IME-SM1	3.28E-12
gp19	hypothetical protein	8518	8726	+	65		
gp20	hypothetical protein	8684	8913	+	73		
gp21	hypothetical protein	8907	9117	+	67	A0A218M346_9VIRU Uncharacterized protein OS=*Acidovorax* phage ACP17	1.83E-12

Table 8. Continued

GP	Name	Start	End	Strand	Length (AA)	Representative homologue	E value
gp22	hypothetical protein	9104	9271	+	51		
gp23	hypothetical protein	9283	9568	+	92		
gp24	hypothetical protein	9992	10399	+	132		
gp25	hypothetical protein	10385	10608	+	71	A0A023NP49_9GAMM Uncharacterized protein OS=*Dyella jiangningensis*	1.85E-05
gp26	hypothetical protein	10594	11132	+	176	A0A0E3FWE4_9CAUD Uncharacterized protein OS=*Synechococcus* phage ACG-2014f	2.37E-06
gp27	hypothetical protein	11137	11449	+	100		
gp28	hypothetical protein	11439	11793	+	114		
gp29	hypothetical protein	11784	11996	+	67	A0A0F9RYF5_9ZZZZ Uncharacterized protein OS=marine sediment metagenome	2.20E-05
tRNA	tRNA-Val	11996	12072	+	0		
tRNA	tRNA-Leu	12078	12155	+	0		
tRNA	tRNA-Leua	12245	12323	+	0		
gp30	hypothetical protein	12314	12505	+	60		
tRNA	tRNA-Thr	12467	12542	+	0		
tRNA	tRNA-Met	12548	12624	+	0		
gp31	hypothetical protein	12629	12892	+	84		
gp32	ribonucleoside-diphosphate reductase subunit alpha	13037	15367	+	773	NP_049845.1 T4_gene_nrdA ribonucleoside-diphosphate reductase subunit alpha, IPR000788	2.54E-167
gp33	hypothetical protein	15320	15515	+	60		
gp34	nrdB aerobic NDP reductase, small subunit	15500	16600	+	363	NP_049841.1 T4_gene_nrdB NrdB aerobic NDP reductase, small subunit, IPR000358	7.14E-64
gp35	hypothetical protein	16563	16967	+	130	IPR021686	1.60E-34
gp36	glutaredoxin	16945	17184	+	75	IPR002109	1.10E-11
gp37	hypothetical protein	17451	18558	+	366	A0A0H4IPU2_9CAUD Uncharacterized protein OS=*Stenotrophomonas* phage IME-SM1	1.28E-29
gp38	hypothetical protein	18604	18812	+	66		
gp39	hypothetical protein	18798	19252	+	148		

Table 8. Continued

GP	Name	Start	End	Strand	Length (AA)	Representative homologue	E value
gp40	hypothetical protein	19271	19792	+	170	A0A218M399_9VIRU Uncharacterized protein OS=*Acidovorax phage* ACP17	2.03E-38
gp41	hypothetical protein	19777	20097	+	103		
gp42	hypothetical protein	20441	20731	+	93		
gp43	DNA ligase	20770	22075	+	432	NP_049813.1 T4_gene_30 DNA ligase, IPR012310	2.24E-63
gp44	hypothetical protein	22173	22443	+	85		
gp45	hypothetical protein	22464	22744	+	90		
gp46	hypothetical protein	22731	22995	+	84		
gp47	hypothetical protein	23007	23304	+	95		
gp48	hypothetical protein	23291	23612	+	103		
gp49	hypothetical protein	23596	24094	+	161		
gp50	hypothetical protein	24090	24543	+	151		
gp51	hypothetical protein	24823	24950	+	39		
tRNA	tRNA-Trp	25058	25132	+	0		
tRNA	tRNA-Cys	25214	25290	+	0		
tRNA	tRNA-Pro	25300	25377	+	0		
gp52	hypothetical protein	25335	25532	+	63		
gp53	hypothetical protein	25573	25737	+	50		
tRNA	tRNA-Ala	25573	25648	+	0		
tRNA	tRNA-Alaa	25654	25730	+	0		
tRNA	tRNA-Leuc	25741	25826	+	0		
gp54	hypothetical protein	25775	25961	+	59		
tRNA	tRNA-Lys	26035	26109	+	0		
tRNA	tRNA-Thra	26115	26191	+	0		
tRNA	tRNA-Gly	26271	26345	+	0		
tRNA	tRNA-Glu	26356	26434	+	0		
tRNA	tRNA-Glua	26440	26515	+	0		
tRNA	tRNA-Arg	26521	26598	+	0		
tRNA	tRNA-Tyra	26608	26694	+	0		

Table 8. Continued

GP	Name	Start	End	Strand	Length (AA)	Representative homologue	E value
tRNA	tRNA-Tyr	26701	26792	+	0		
tRNA	tRNA-Vala	26800	26875	+	0		
tRNA	tRNA-Gluc	27925	28003	+	0		
tRNA	tRNA-Proa	28245	28322	+	0		
tRNA	tRNA-Asn	28330	28416	+	0		
tRNA	tRNA-Asna	28421	28497	+	0		
tRNA	tRNA-Asp	28506	28581	+	0		
tRNA	tRNA-Aspa	28589	28667	+	0		
tRNA	tRNA-Meta	28761	28836	+	0		
tRNA	tRNA-Lysa	28924	29000	+	0		
tRNA	tRNA-Lysc	29084	29172	+	0		
gp55	hypothetical protein	29176	29467	+	94	A0A218M301_9VIRU Uncharacterized protein OS=*Acidovorax* phage ACP17	1.25E-04
gp56	hypothetical protein	29473	29693	+	70		
tRNA	tRNA-Lys|Stop	29702	29776	+	0		
gp57	ribonuclease H-like	29850	30336	+	158	IPR007405	6.90E-14
tRNA	tRNA-Leud	30342	30428	+	0		
tRNA	tRNA-Phe	30435	30511	+	0		
gp58	hypothetical protein	30563	30762	+	62		
tRNA	tRNA-Phea	30785	30860	+	0		
gp59	GroES molecular chaperone protein	30865	31124	+	83	A0A142F037_9VIRU GroES molecular chaperone protein OS=*Stenotrophomonas* phage vB_SmaS-DLP_6	2.78E-14
tRNA	tRNA-His	31138	31215	+	0		
tRNA	tRNA-Ile	31223	31298	+	0		
tRNA	tRNA-Ilea	31305	31379	+	0		
tRNA	tRNA-Gln	31576	31651	+	0		
tRNA	tRNA-Glna	31658	31732	+	0		
gp60	hypothetical protein	31987	32109	+	35		
gp61	hypothetical protein	32176	32469	+	95		

Table 8. Continued

GP	Name	Start	End	Strand	Length (AA)	Representative homologue	E value
gp62	hypothetical protein	32577	32713	+	41		
gp63	hypothetical protein	32706	32947	+	77		
gp64	hypothetical protein	32931	33261	+	107		
gp65	hypothetical protein	33252	33365	+	33		
gp66	hypothetical protein	33364	33548	+	58		
gp67	hypothetical protein	33596	34072	+	156		
gp68	hypothetical protein	34058	34428	+	119	A0A142F006_9VIRU Uncharacterized protein OS=*Stenotrophomonas* phage vB_SmaS-DLP_6	2.06E-05
gp69	hypothetical protein	34418	34655	+	75		
gp70	hypothetical protein	34614	34807	+	60		
tRNA	tRNA-Ser	34770	34857	+	0		
gp71	hypothetical protein	34861	35334	+	154	A0A142EZW0_9VIRU Uncharacterized protein OS=Stenotrophomonas phage vB_SmaS-DLP_6	1.39E-24
gp72	hypothetical protein	35436	35640	+	65		
tRNA	tRNA-Thrc	35630	35705	+	0		
gp73	hypothetical protein	35769	35910	+	42		
tRNA	tRNA-Glya	35887	35964	+	0		
gp74	hypothetical protein	36034	36522	+	159		
gp75	hypothetical protein	36514	36846	+	108		
gp76	hypothetical protein	36902	37181	+	88		
gp77	hypothetical protein	37164	37471	+	98		
gp78	hypothetical protein	37454	37761	+	98		
gp79	hypothetical protein	37746	38051	+	97		
gp80	hypothetical protein	38031	38329	+	94		
gp81	calcineurin-like phosphoesterase	38296	39083	+	259		
gp82	hypothetical protein	39067	39439	+	120	F8SJR6_9CAUD Uncharacterized protein 034 OS=*Pseudomonas* phage PhiPA3	3.75E-15

Table 8. Continued

GP	Name	Start	End	Strand	Length (AA)	Representative homologue	E value
gp83	hypothetical protein	39426	39588	+	50		
gp84	hypothetical protein	39580	40572	+	327	A0A0H4IP63_9CAUD Uncharacterized protein OS=*Stenotrophomonas* phage IME-SM1	1.79E-32
gp85	hypothetical protein	40558	40901	+	111		
gp86	hypothetical protein	40892	41148	+	82		
gp87	hypothetical protein	41265	41929	+	217	|A0A0H4INV0_9CAUD Uncharacterized protein OS=*Stenotrophomonas* phage IME-SM1	2.33E-17
gp88	phosphohydrolase	42049	42562	+	168	A0A0H4IS72_9CAUD Phosphohydrolase OS=*Stenotrophomonas* phage IME-SM1	1.02E-45
gp89	hypothetical protein	42541	43007	+	152		
gp90	hypothetical protein	43007	43240	+	74	A0A142EZZ3_9VIRU Uncharacterized protein OS=*Stenotrophomonas* phage vB_SmaS-DLP_6	3.72E-14
gp91	hypothetical protein	43271	43434	+	49		
gp92	DNA topoisomerase II large subunit	43522	45344	+	604	NP_049621.1 T4_gene_39 DNA topoisomerase II large subunit , IPR001241	8.35E-51
gp93	DNA topisomerase II medium subunit	45331	46705	+	455	NP_049875.1 T4_gene_52 DNA topisomerase II medium subunit , IPR002205	3.06E-57
gp94	hypothetical protein	46757	47086	+	106		
gp95	hypothetical protein	47072	47355	+	91		
gp96	hypothetical protein	47341	47651	+	100		
gp97	hypothetical protein	47644	47874	+	72		
gp98	hypothetical protein	47863	48172	+	98		
gp99	hypothetical protein	48153	48525	+	119	A0A292GJA5_9VIRU Predicted ORF OS=*Xanthomonas* phage XacN1	1.12E-09
gp100	hypothetical protein	48534	49002	+	152	A0A142IDS7_9CAUD Uncharacterized protein OS=*Pseudomonas* phage vB_PsyM_KIL1	1.40E-13
gp101	polynucleotide kinase	48988	49892	+	297	NP_049834.1 T4_gene_pseT polynucleotide kinase	1.52E-42
gp102	hypothetical protein	49883	50202	+	103		

Table 8. Continued

GP	Name	Start	End	Strand	Length (AA)	Representative homologue	E value
gp103	hypothetical protein	50172	50404	+	73		
gp104	hypothetical protein	50464	51470	+	330	A0A218M383_9VIRU Uncharacterized protein OS=*Acidovorax* phage ACP17	4.06E-115
gp105	hypothetical protein	51469	51726	+	82	A0A142F064_9VIRU Uncharacterized protein OS=*Stenotrophomonas* phage vB_SmaS-DLP_6	1.53E-06
gp106	hypothetical protein	51877	52128	+	80		
gp107	hypothetical protein	52113	52418	+	98		
gp108	hypothetical protein	52410	52819	+	133	A0A218M324_9VIRU Uncharacterized protein OS=*Acidovorax* phage ACP17	2.85E-35
gp109	hypothetical protein	52811	53083	+	85		
gp110	hypothetical protein	53064	53259	+	60		
gp111	hypothetical protein	53243	53534	+	93		
gp112	hypothetical protein	53521	53923	+	131		
gp113	hypothetical protein	53907	54135	+	72		
gp114	hypothetical protein	54107	54322	+	66		
gp115	hypothetical protein	54307	54509	+	62		
gp116	hypothetical protein	54552	54976	+	137		
gp117	hypothetical protein	54975	55163	+	59		
gp118	hypothetical protein	55150	55525	+	121	A0A142F003_9VIRU Uncharacterized protein OS=*Stenotrophomonas* phage vB_SmaS-DLP_6	6.70E-13
gp119	hypothetical protein	55512	55716	+	65		
gp120	hypothetical protein	55698	56255	+	181	A0A0H4INI0_9CAUD Uncharacterized protein OS=*Stenotrophomonas* phage IME-SM1	2.73E-05
gp121	hypothetical protein	56245	56547	+	97		
gp122	FAD-dependent thymidylate synthase	56548	57530	+	324	A0A142EZP7_9VIRU FAD-dependent thymidylate synthase OS=*Stenotrophomonas* phage vB_SmaS-DLP_6 , IPR003669	1.07E-146
gp123	hypothetical protein	57507	57798	+	94		
gp124	hypothetical protein	57782	57992	+	66	A0A142EZP7_9VIRU FAD-dependent thymidylate synthase OS=*Stenotrophomonas* phage vB_SmaS-DLP_6 , IPR003669	

Table 8. Continued

GP	Name	Start	End	Strand	Length (AA)	Representative homologue	E value
gp125	hypothetical protein	57968	58323	+	114		
gp126	hypothetical protein	58307	58721	+	134		
gp127	hypothetical protein	58706	59014	+	99		
gp128	hypothetical protein	59003	59289	+	92	IPR025109	3.60E-30
gp129	hypothetical protein	59273	59558	+	91	A0A1B2IGA5_9CAUD Uncharacterized protein OS=*Erwinia* phage vB_EamM_Phobos	1.46E-06
gp130	hypothetical protein	59529	59773	+	77		
gp131	6-pyruvoyl tetrahydropterin synthase	59789	60308	+	169	IPR007115	2.20E-14
gp132	hypothetical protein	60313	61040	+	239		
gp133	hypothetical protein	61143	61616	+	154		
gp134	hypothetical protein	61650	61877	+	72		
gp135	hypothetical protein	61863	62224	+	116		
gp136	hypothetical protein	62227	62717	+	160	E5E470_9CAUD Uncharacterized protein OS=*Acinetobacter* phage Acj6	1.40E-14
gp137	hypothetical protein	62803	63047	+	76		
gp138	hypothetical protein	63040	63412	+	121		
gp139	RNA ligase	63411	64588	+	389	IPR021122	2.90E-15
gp140	hypothetical protein	64574	64953	+	123	B2ZXP5_9CAUD Uncharacterized protein OS=*Ralstonia* phage phiRSL1	9.36E-08
gp141	YbiA-like protein	64934	65408	+	153	IPR012816	5.40E-24
gp142	hypothetical protein	65386	65760	+	121		
gp143	hypothetical protein	65746	65948	+	64		
gp144	hypothetical protein	65965	66171	+	65	W8EDH1_9CAUD Uncharacterized protein OS=*Pseudomonas* phage phiPsa374	1.81E-05
gp145	hypothetical protein	66160	66395	+	75		
gp146	hypothetical protein	66565	66779	+	67		
gp147	hypothetical protein	67074	67671	+	196		
gp148	hypothetical protein	67662	68313	+	213		
gp149	hypothetical protein	68295	68978	+	223		

Table 8. Continued

GP	Name	Start	End	Strand	Length (AA)	Representative homologue	E value
gp150	tail fiber protein	68978	70724	+	579	A0A031IUV4_9PSED Phage-related tail fiber protein-like protein OS=*Pseudomonas* sp. RIT357	2.48E-21
gp151	tail fiber protein	70800	74954	+	1381	A0A142EZL1_9VIRU Tail fiber protein OS=*Stenotrophomonas* phage vB_SmaS-DLP_6	2.35E-167
gp152	hypothetical protein	74938	75352	+	134	A0A142EZY6_9VIRU Uncharacterized protein OS=*Stenotrophomonas* phage vB_SmaS-DLP_6	1.13E-47
gp153	hypothetical protein	75342	75840	+	163		
gp154	hypothetical protein	75877	76273	+	128		
gp155	hypothetical protein	76267	76521	+	82		
gp156	endolysin A	76506	77165	+	214	ENLYS_BPMD2 Endolysin A OS=*Mycobacterium* phage D29	6.18E-09
gp157	hypothetical protein	77157	77483	+	105		
gp158	Cell wall hydrolase	77599	78208	+	199	IPR011105	2.70E-26
gp159	hypothetical protein	78238	78449	+	67		
gp160	RNA ligase A	78467	79595	+	372	NP_049839.1 T4_gene_rnlA RNA ligase A, IPR019039	3.96E-24
gp161	hypothetical protein	79583	79792	+	66		
gp162	hypothetical protein	79997	80223	+	71	A0A0E3JI93_9CAUD Uncharacterized protein OS=*Rhodoferax* phage P26218	3.20E-13
gp163	hypothetical protein	80222	80544	+	103		
gp164	hypothetical protein	80531	80669	+	42		
gp165	hypothetical protein	80662	80817	+	48		
gp166	hypothetical protein	80801	81074	+	87		
gp167	hypothetical protein	81058	81310	+	80		
gp168	hypothetical protein	81278	81677	+	129		
gp169	hypothetical protein	81661	81826	+	51		
gp170	hypothetical protein	81812	82143	+	106		
gp171	hypothetical protein	82225	82549	+	104		
gp172	hypothetical protein	82657	83045	+	125		
gp173	hypothetical protein	83044	83450	+	132		

Table 8. Continued

GP	Name	Start	End	Strand	Length (AA)	Representative homologue	E value
gp174	hypothetical protein	83440	83647	+	66		
gp175	hypothetical protein	83634	83928	+	95		
gp176	tRNA nucleotidyl transferase	83912	84998	+	357	A0A292GDU1_9VIRU CCA tRNA nucleotidyl transferase OS=*Xanthomonas* phage XacN1	3.42E-116
gp177	hypothetical protein	84978	85365	+	125		
gp178	hypothetical protein	86106	86335	+	72		
gp179	hypothetical protein	86380	87028	-	213	A0A218M3F0_9VIRU Uncharacterized protein OS=*Acidovorax* phage ACP1	4.24E-55
gp180	DNA end protector protein	87015	87633	-	202	NP_049754.1 T4_gene_2 DNA end protector protein	1.29E-16
gp181	head completion protein	87624	88093	-	152	NP_049755.1 T4_gene_4 head completion protein	6.57E-34
gp182	hypothetical protein	88150	88284	-	39		
gp183	baseplate tail tube cap	88356	89081	+	237	A0A0H4ISA7_9CAUD Putative tail tube associated base plate protein OS=*Stenotrophomonas* phage IME-SM1	7.84E-69
gp184	baseplate wedge subunit	89068	89622	+	180	NP_049756.1 T4_gene_53 baseplate wedge subunit, IPR022607	3.39E-06
gp185	hypothetical protein	89609	90848	+	410	A0A0H4J2I9_9CAUD Uncharacterized protein OS=*Stenotrophomonas* phage IME-SM1	1.39E-157
gp186	baseplate central spike complex protein	90909	92313	+	465	NP_049757.1 T4_gene_5 baseplate hub subunit and tail lysozyme, IPR009590	3.08E-22
gp187	hypothetical protein	92478	92924	+	144	A0A223AIZ9_9VIRU Uncharacterized protein OS=*Acidovorax* phage ACP17	3.95E-61
gp188	hypothetical protein	92983	93415	-	140		
gp189	hypothetical protein	93413	93896	-	157	IPR025358	5.40E-24
gp190	hypothetical protein	93925	94342	-	135		
gp191	hypothetical protein	94319	94569	-	79		
gp192	hypothetical protein	94694	94951	-	82	A0A0H4ISC1_9CAUD Uncharacterized protein OS=*Stenotrophomonas* phage IME-SM1	6.17E-04
gp193	hypothetical protein	95056	95289	-	74		
gp194	hypothetical protein	95282	95500	-	67		

Table 8. Continued

GP	Name	Start	End	Strand	Length (AA)	Representative homologue	E value
gp195	hypothetical protein	95479	96297	-	269	A0A292GL82_9VIRU DUF4343 domain containing protein OS=*Xanthomonas* phage XacN1, IPR025643	2.90E-110
gp196	flotillin-like protein	96354	97734	-	455	A0A1H0ZF08_9GAMM Flotillin OS=Pseudoxanthomonas sp. CF125 , IPR027705	8.57E-169
gp197	hypothetical protein	97718	98297	-	190	Q7Y4Z4_BPR69 Uncharacterized protein OS=*Enterobacteria* phage RB69	3.69E-04
gp198	hypothetical protein	98287	98583	-	94		
gp199	hypothetical protein	98565	98983	-	136		
gp200	hypothetical protein	98972	99393	-	137	A0A024AZ34_9CAUD Uncharacterized protein OS=*Bacillus* phage CAM003	1.18E-20
gp201	hypothetical protein	99392	99788	-	129		
gp202	hypothetical protein	99765	100011	-	77		
gp203	hypothetical protein	100013	100220	-	69		
gp204	hypothetical protein	100224	100456	-	74		
gp205	hypothetical protein	100442	100676	-	74		
gp206	hypothetical protein	100660	101013	-	112		
gp207	hypothetical protein	101051	102898	+	612	A0A0H4ISB2_9CAUD Uncharacterized protein OS=*Stenotrophomonas* phage IME-SM1	8.65E-168
gp208	hypothetical protein	102883	103827	+	310	A0A239NNH2_9GAMM Uncharacterized protein OS=*Stenotrophomonas* sp. YR34	1.06E-24
gp209	hypothetical protein	103822	104813	+	325		
gp210	hypothetical protein	104828	105248	+	136		
gp211	hypothetical protein	105290	106528	+	408		
gp212	concanavalin A-like lectin/glucanase domain superfamily	106518	108927	+	800	IPR013320	3.82E-22
gp213	hypothetical protein	109008	112214	+	1065	A0A218M2T2_9VIRU Uncharacterized protein OS=*Acidovorax* phage ACP17	4.17E-51
gp214	hypothetical protein	112433	113539	+	365	A0A0H4ISB7_9CAUD Uncharacterized protein OS=*Stenotrophomonas* phage IME-SM1	1.30E-103

Table 8. Continued

GP	Name	Start	End	Strand	Length (AA)	Representative homologue	E value
gp215	hypothetical protein	113747	114049	+	95	NP_049763.1 T4_gene_5.4 gp5.4 conserved hypothetical protein, IPR008727	1.73E-05
gp216	baseplate wedge subunit	114107	114438	+	107	IPR007048	3.10E-06
gp217	baseplate wedge subunit	114423	116204	+	590	NP_049764.1 T4_gene_6 baseplate wedge subunit	7.55E-30
gp218	hypothetical protein	116187	117697	+	499	A0A0H4ITL7_9CAUD Uncharacterized protein OS=*Stenotrophomonas* phage IME-SM1	2.15E-171
gp219	baseplate wedge subunit	117695	119232	+	508	IPR015298	7.32E-16
gp220	hypothetical protein	119231	122489	+	1083	IPR032096	1.50E-16
gp221	hypothetical protein	122494	125035	+	844	A0A1S5R3Y8_9VIRU Uncharacterized protein OS=*Pseudomonas* phage pf16	5.70E-28
gp222	hypothetical protein	125076	125235	+	50		
gp223	neck protein	125367	126141	+	255	NP_049772.1 T4_gene_13 neck protein	2.82E-22
gp224	neck protein	126163	126819	+	215	NP_049773.1 T4_gene_14 neck protein, IPR021674	5.24E-17
gp225	tail sheath stabilizer and completion protein	126807	127559	+	247	NP_049774.1 T4_gene_15 tail sheath stabilizer and completion protein, IPR031997	2.01E-17
gp226	hypothetical protein	127550	127841	+	93		
gp227	small terminase subunit	127829	128350	+	170	NP_049775.1 T4_gene_16 small terminase protein, IPR020342	1.67E-07
gp228	large terminase subunit	128839	130498	+	550	NP_049777.1 T4_gene_17 large terminase protein, IPR004921	2.04E-118
gp229	tail sheath protein	130555	132544	+	659	NP_049780.1 T4_gene_18 tail sheath protein, IPR007067	8.64E-80
gp230	hypothetical protein	132620	133081	+	150		
gp231	tail tube protein	133145	133706	+	183	NP_049781.1 T4_gene_19 tail tube protein, IPR010667	1.70E-20
gp232	portal protein	133778	135456	+	556	NP_049782.1 T4_gene_20 portal vertex protein, IPR010823	1.93E-98
gp233	putative prohead core protein	135443	136250	+	265	A1XGY5_9CAUD GP68-prohead core protein OS=Stenotrophomonas phage Smp14	5.45E-76

Table 8. Continued

GP	Name	Start	End	Strand	Length (AA)	Representative homologue	E value
gp234	hypothetical protein	136235	136495	+	82		
gp235	prohead core scaffolding protein protease	136500	137203	+	230	NP_049785.1 T4_gene_21 prohead core scaffolding protein and protease , IPR005082	1.17E-18
gp236	prohead core protein	137257	138078	+	270	NP_049786.1 T4_gene_22 prohead core protein	1.27E-05
gp237	major capsid protein	138135	139384	+	412	NP_049787.1 T4_gene_23 major capsid protein, IPR010762	1.49E-77
gp238	hypothetical protein	139745	140029	+	91		
gp239	deoxynucleoside monophosphate kinase	140016	140571	+	182	NP_049752.1 T4_gene_1 deoxynucleoside monophosphate kinase	2.28E-18
gp240	tail completion and sheath stabilizer protein	140579	141062	+	161	NP_049753.1 T4_gene_3 tail completion and sheath stabilizer protein	2.88E-13
gp241	UvsY recombination, repair and ssDNA binding protein	141035	141474	+	142	NP_049799.2 T4_gene_uvsY UvsY recombination, repair and ssDNA binding protein , IPR021289	1.08E-07
gp242	homing endonuclease	141501	142066	+	185	A0A0B5H2A1_9CAUD Homing endonuclease OS=Salmonella phage Mushroom	1.78E-06
gp243	UvsW helicase	142059	143568	+	500	NP_049796.1 T4_gene_uvsW UvsW helicase	1.52E-91
gp244	hypothetical protein	143519	143987	+	153		
gp245	RNA polymerase sigma factor	144003	144483	+	160	NP_049679.1 T4_gene_55 RNA polymerase sigma factor	1.26E-13
gp246	endonuclease subunit	144481	145554	+	354	NP_049672.1 T4_gene_47 endonuclease subunit	6.44E-38
gp247	hypothetical protein	145541	145772	+	74		
gp248	recombination endonuclease subunit	145756	147487	+	573	NP_049669.1 T4_gene_46 endonuclease subunit, IPR003395	1.03E-84
gp249	hypothetical protein	147466	147711	+	76		
gp250	hypothetical protein	147706	147882	+	55		
gp251	sliding clamp	147948	148601	+	213	NP_049666.1 T4_gene_45 sliding clamp	1.25E-18
gp252	hypothetical protein	148589	149022	+	140		
gp253	clamp loader small subunit	149035	149992	+	315	NP_049665.1 T4_gene_44 clamp loader, small subunit	1.21E-45
gp254	clamp loader A subunit	149998	150414	+	135	NP_049664.1 T4_gene_62 clamp loader small subunit , IPR031868	2.86E-07

Table 8. Continued

GP	Name	Start	End	Strand	Length (AA)	Representative homologue	E value
gp255	translation repressor RegA	150371	150808	+	142	NP_049663.1 T4_gene_regA translation repressor protein , IPR002702	2.24E-29
gp256	deoxyuridine-triphosphatase	150781	151448	+	218	IPR008180	2.40E-19
gp257	hypothetical protein	151437	151735	+	96	A0A0H4ITP8_9CAUD Uncharacterized protein OS=*Stenotrophomonas* phage IME-SM1	2.70E-13
gp258	hypothetical protein	151806	151943	+	42		
gp259	DNA polymerase	152076	154772	+	894	NP_049662.1 T4_gene_43 DNA polymerase, IPR006134	5.72E-113
gp260	hypothetical protein	154772	155143	+	120		
gp261	UvsX RecA-like recombination protein	155127	156195	+	352	NP_049656.2 T4_gene_uvsX UvsX RecA-like recombination protein, IPR013765	3.17E-121
gp262	hypothetical protein	156179	157160	+	322	A0A0H4ITQ9_9CAUD Uncharacterized protein OS=*Stenotrophomonas* phage IME-SM1	8.61E-14
gp263	hypothetical protein	157145	157435	+	92		
gp264	GTP cyclohydrolase I	157458	158153	+	228	IPR020602	8.30E-53
gp265	phosphoadenosine phosphosulphate reductase	158145	158694	+	180	IPR002500	1.90E-05
gp266	hypothetical protein	158701	159349	+	216		
gp267	hypothetical protein	159325	159773	+	144		
gp268	glycosyl transferase	159755	160927	+	386	IPR001296	6.10E-12
gp269	hypothetical protein	160920	162242	+	438	A0A218M2Y9_9VIRU Uncharacterized protein OS=*Acidovorax* phage ACP17	9.92E-47
gp270	hypothetical protein	162298	162684	+	124		
gp271	queuosine biosynthesis QueE radical SAM	162669	163577	+	298	A0A0H4ITQ6_9CAUD Queuosine biosynthesis QueE radical SAM OS=*Stenotrophomonas* phage IME-SM1	2.64E-134
gp272	hypothetical protein	163660	163882	+	70		
gp273	hypothetical protein	163864	164073	+	65		
gp274	hypothetical protein	164054	164225	+	52		

Table 8. Continued

GP	Name	Start	End	Strand	Length (AA)	Representative homologue	E value
gp275	hypothetical protein	164209	164659	+	146	A0A2D1GNA1_9VIRU Uncharacterized protein OS=*Pseudoalteromonas* phage J2-1	7.36E-23
gp276	ATP-dependent DNA helicase	164645	166059	+	468	NP_049654.1 T4_gene_41 41 helicase	6.73E-107
gp277	hypothetical protein	166043	166307	+	83		
gp278	hypothetical protein	166556	167585	-	340	NP_049708.1 T4_gene_nrdC.10 NrdC.10 conserved hypothetical protein	1.27E-70
gp279	hypothetical protein	167682	168758	+	356	A0A0H4J2Q0_9CAUD Uncharacterized protein OS=*Stenotrophomonas* phage IME-SM1	4.03E-12
gp280	hypothetical protein	168746	169759	+	334		
gp281	hypothetical protein	169746	170616	+	287		
gp282	phosphopantetheine adenylyltransferase	170598	171097	+	163	COAD_PROA2 Phosphopantetheine adenylyltransferase OS=*Prosthecochloris aestuarii* (strain DSM 271 / SK 413)	8.64E-09
gp283	hypothetical protein	171078	171320	+	77		
gp284	hypothetical protein	171313	172212	+	297		
gp285	hypothetical protein	172190	172621	+	139	A0A218M349_9VIRU Uncharacterized protein OS=Acidovorax phage ACP17	2.96E-41
gp286	baseplate hub subunit	172615	173409	+	261	NP_049801.1 T4_gene_26 gp26 baseplate hub subunit	2.02E-04
gp287	hypothetical protein	173569	175809	+	744	IPR023346	8.44E-14
gp288	i-spanin	175801	176379	-	189		
gp289	o-spanin	175860	176157	-	90		
gp290	hypothetical protein	176367	176758	-	127	A0A218M2Z8_9VIRU Uncharacterized protein OS=*Acidovorax* phage ACP17	5.11E-18
gp291	hypothetical protein	176757	177264	-	165		
gp292	DNA primase	177365	178334	+	318	NP_049648.1 T4_gene_61 DNA primase	6.72E-43
gp293	PhoH-like protein	178324	179044	+	237	IPR003714	9.50E-41
gp294	hypothetical protein	179042	179256	+	68		
gp295	hypothetical protein	179245	179442	+	61		
gp296	RnaseH	179435	180308	+	288	NP_049859.1 T4_gene_rnh RnaseH, IPR020045	9.52E-41

Table 8. Continued

GP	Name	Start	End	Strand	Length (AA)	Representative homologue	E value
gp297	putative regulatory protein, FmdB	180292	180564	+	85	IPR013429	1.30E-09
gp298	hypothetical protein	180553	180839	+	92		
gp299	restriction endonuclease type II-like	180818	181491	+	220	IPR015085	9.92E-06
gp300	hypothetical protein	181473	181733	+	82		
gp301	hypothetical protein	181720	181954	+	75		
gp302	T4-like gp59 loader of DNA helicase	182020	182547	+	172	NP_049856.1 T4_gene_59 59 protein, IPR015085	5.14E-08
gp303	single-stranded DNA binding protein	182587	183510	+	304	NP_049854.1 T4_gene_32 single-stranded DNA binding protein , IPR012339	1.07E-37
gp304	poly(ADP-ribose) polymerase	183707	187765	+	1347	IPR012317	5.90E-08
gp305	exoribonuclease	187829	188474	+	212	NP_049629.1 T4_gene_dexA exonuclease, IPR033390	2.55E-29
gp306	hypothetical protein	188463	188876	+	134	A0A142EZY4_9VIRU Uncharacterized protein OS=*Stenotrophomonas* phage vB_SmaS-DLP_6	5.52E-11
gp307	hypothetical protein	188923	189169	+	78		
gp308	hypothetical protein	189164	189363	+	63		
gp309	hypothetical protein	189359	189599	+	80		
gp310	hypothetical protein	189574	189909	+	108		
gp311	hypothetical protein	189888	190072	+	57		
gp312	hypothetical protein	190050	190253	+	63		
gp313	hypothetical protein	190240	190615	+	121		
gp314	hypothetical protein	190591	190880	+	91		
gp315	hypothetical protein	190852	191154	+	97	A0A0H4INW9_9CAUD Uncharacterized protein OS=*Stenotrophomonas* phage IME-SM1	5.43E-11
gp316	hypothetical protein	191112	191326	+	68	A0A142F092_9VIRU Uncharacterized protein OS=*Stenotrophomonas* phage vB_SmaS-DLP_6	2.67E-11
gp317	hypothetical protein	191319	191457	+	43		
gp318	hypothetical protein	191628	192039	+	133		

Table 8. Continued

GP	Name	Start	End	Strand	Length (AA)	Representative homologue	E value
gp319	hypothetical protein	192113	192298	+	58		
gp320	hypothetical protein	192346	192798	+	147		
gp321	hypothetical protein	192842	193121	+	93		
gp322	Cytidyltransferase-like protein	193138	194268	+	373	IPR005123	1.00E-06
gp323	oxoglutarate/iron-dependent dioxygenase	194239	194980	+	242	IPR005123	5.40E-10
gp324	NAD/GMP synthase	194972	195815	+	277	IPR022310	2.30E-29
gp325	hypothetical protein	195858	197010	+	381	A0A292GJP9_9VIRU Uncharacterized protein OS=*Xanthomonas* phage XacN1	3.33E-119
gp326	hypothetical protein	197034	197643	+	199	A0A191ZBT9_9CAUD Uncharacterized protein OS=*Erwinia* phage vB_EamM_Special G	1.12E-41
gp327	ADP-ribose pyrophosphatase	197723	198779	+	348	A0A142EZP1_9VIRU ADP-ribose pyrophosphatase OS=*Stenotrophomonas* phage vB_SmaS-DLP_6	8.19E-127
gp328	hypothetical protein	198777	199186	+	132		

[a] GP = Gene products
[b] AA = Amino acid

CHAPTER III

RECEPTOR SITE IDENTIFICATION

Introduction

Adsorption is a key step in the phage infection process. A phage cannot infect its host if the receptor becomes inaccessible or non-complementary to the phage receptor-binding proteins (Bertozzi Silva et al., 2016). Receptor identification is very important because mutational receptor loss is one common cause of phage resistance (Levin and Bull, 2004). My objective is to identify the receptor site(s) for the three characterized virulent phages of *Xac*. A comparison of the genome sequence of a phage-sensitive wild type strain to that of a phage resistant mutants can help to identify the site of the mutation that confers resistance, and thus possibly the receptor. Another approach can be a rational selection of potential phage receptors. Since it is known that twitching motility, biofilm formation, adherence and infection by an uncharacterized phage of *Xac* are mediated by type IV pili (T4P) (Dunger et al., 2014), a deletion mutation in the major pilus subunit gene *pilA* is a rational approach.

Materials and methods

Bacterial strains and plasmids conditions

Bacterial strains and plasmids used in this study are listed in Table 9. *Xac* strains were cultured at 28ºC in MNBY broth or agar plates. For *Xac* cultures harboring plasmids, MNBY medium was supplemented with kanamycin (Km, 30 µg/ml). Yeast tryptone broth (YTB: 10 g/liter tryptone, 10 g/liter yeast extract) and yeast-tryptone agar amended with sucrose [YTSA; YTB amended with 20 g/liter, sucrose final concentration 15% (wt/vol)]

were used for resolution of mutants. *Escherichia coli* strains were cultured at 37°C in LB broth or LB agar (Bertani, 1951). For *E. coli* cultures harboring plasmids, LB medium was supplemented with Km (30 µg/ml).

Table 9. Bacterial strains and plasmids used in this study.

Strain or plasmid	Genotype and relevant features[a]	Reference
Xanthomonas		
EC-12	*Xanthomonas* sp., rice isolate (ATCC PTA-13101)	(Ahern et al., 2014)
Block 22	*X. axonopodis* pv. *citri*, sweet orange isolate	Wang, N.[b]
Block 22-*ΔpilA*	Block 22, unmarked deletion of *pilA*	This study
Block 22-Comp	Block 22, pMo168::*pilA*	This study
E. coli		
E. cloni 5-alpha	*fhuA2*Δ(*argF-lacZ*)*U169 phoA glnV44* Φ80Δ(*lacZ*)M15 *gyrA96 recA1 relA1 endA1 thi-1 hsdR17*	Lucigen
Plasmids		
pMo130	Suicide vector for allelic exchange; ColE1 *ori*, RK2 *oriT*, *xylE*, *sacB*, Km^r	(Hamad et al., 2009)
pMo130::*pilA*	pM0130 with *pilA* upstream and downstream fragments	This study
pMo168	Replicative vector; *ori* pBBR1, mob^+, *xylE*, Km^r	(Hamad et al., 2009)
pMo168::*pilA* comp	*pilA* clones into pMo168	This study

[a] Km^r = resistance to kanamycin.
[b] University of Florida

Construction of Xac Block 22 pilA deletion and in-trans complementation

The system developed by Hamad *et al.* (Hamad et al., 2009) with modifications was used to construct deletion and complementation in genes of interest (Figure 9).

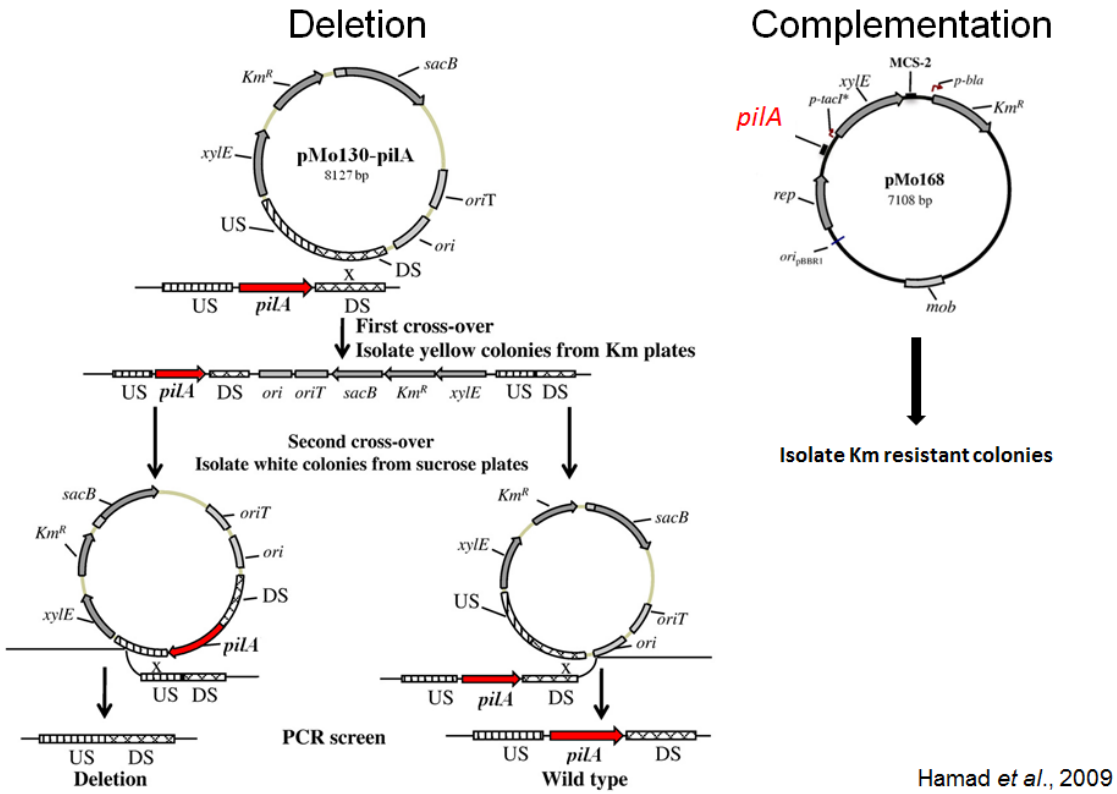

Figure 9. Strategy for Type IV pili gene deletion and complementation of *Xac* (Figure adapted from Hamad et al., 2009 with modification, with permission).

PCR primers for regions flanking *pilA* (*XAC3241*) were designed based on the annotated sequence of *Xac* 306 reference genome (Accession: GCA_000007165.1). All plasmid constructs used in this study were generated using *E. coli* E. cloni 5-alpha (Lucigen) as host. Plasmids pMo130 and pMo168 were used in this study. Plasmid pMo130, a suicide vector, carries a ColE1 origin of replication derived from pUC19 and can be used for allelic exchange to generate in-frame deletions in bacterial genome. Plasmid pMo168, a replicative vector, carries the PBBR1 origin of replication and can be used for *in-trans* complementation or gene expression in bacteria. Both plasmids carry an origin of transfer that aid their mobilization into the pathogen through conjugation. Both plasmids also carry reporter *xylE* which encoded a catechol-2,3-dioxygenase, an enzyme

that turns a colorless catechol substrate (pyrocatechol) into a bright yellow-colored 2-hydroxymuconic semialdehyde (Lee et al., 1996).

In order to construct the plasmid pMo130::*pilA* used in the deletion of *pilA* from the Block 22 strain, one kb fragment upstream of the *pilA* was amplified using Δ*pilA*-US-F and Δ*pilA*-US-R primers set (Table 4), digested with NheI and BglII and cloned into multiple cloning sites (MSC) 1 of plasmid pMo130, to obtain pMo130::*pilA*-up. The one kb fragment downstream of *pilA* was amplified using Δ*pilA*-DS-F and Δ*pilA*-DS-R primers set (Table 4). The PCR product was digested with BglII and HindIII, then cloned into pMo130::*pilA*-up to generate pMo130::*pilA.* Plasmid pMo130::*pilA* was introduced into electro-competent cells of Block 22 by electroporation (White and Gonzalez, 1995). Cells were allowed to recover in MNBY broth at 28ºC for 5 h with constant shaking (120 rpm). After incubation, 50, 100, and 150 µl of cells were plated to MNBY Km plates (30 µg/ml). After 72 h, the resulting colonies were sprayed with 0.45 M pyrocatechol to identify colonies in which single crossover events had occurred. Single yellow colonies were grown in YTB for 9 h then spread onto YTSA plates for selection of resolved co-integrants. The colonies that grew on YTSA were sprayed with 0.45 M pyrocatechol. To confirm *pilA* deletion, the presumptive resolved co-integrants exhibiting a white phenotype were analyzed by PCR using multiple primer combinations both internal and external to the target gene deletion and by sequencing of PCR product as well. The deletion mutants were also evaluated for phage activities.

To complement the Block 22-*ΔpilA* mutant, the wild-type *pilA* gene was introduced using a derivative of the plasmid pMo168. The *pilA* gene containing its regulatory region was amplified from Block 22 genomic DNA using *pilA*-comp-F and *pilA*-comp-R primers

set (Table 10). The PCR product was digested with PstI and XbaI, and then cloned into pMo168 MCS-2, resulting in pMo168::*pilA*. The pMo168::*pilA* plasmid was introduced into Block 22-*ΔpilA* by electroporation as described above and plated to MNBY Km plates (30 µg/ml) for selection. Transformants were sprayed with 0.45 M pyrocatechol to identify colonies that contained the pMo168 derivative plasmid. The presence of the wild-type *pilA* gene was confirmed in transformants by PCR amplification and sequencing of PCR product. The complements were evaluated for restoration of phage sensitivity.

Table 10. Primers used in Chapter III for cloning experiments.

Primer	Sequence[a]	Reference
Δ*pilA*-US-F	5'-GAGAGCTAGCGATTGCACTGACCAACATCG-3'	This study
Δ*pilA*-US-R	5'-GAGAGATCTACCCTGTTGCTTCTTCATGG-3'	This study
Δ*pilA*-DS-F	5'-CTCTAGATCTTGCCAGTAATATTTGAACGTTTC-3'	This study
Δ*pilA*-DS-R	5'-CTCTAAGCTTGATTGCTCACCCCTACGAAC-3'	This study
pilA-comp-F	5'-GAGCTGCAGGGGATATCCATGAAGAAGCA-3'	This study
pilA-comp-R	5'-GAGTCTAGAGGAAGCAAGCACCGCGATTA-3'	This study
pilA-U-F	5'-GATCGCAGTTCTTGTGTTTGCCTC-3'	This study
pilA-M-R	5'-CCAACACCGTAATCGCAGAAC-3'	This study
pilA-M-F	5'-GTTCTGCGATTACGGTGTTGG-3'	This study
pilA-M-R	5'-GGAAGCAAGCACCGCGATTA-3'	This study

[a] Added restriction sites are underlined

Isolation and characterization of phage resistant mutants

Xac isolates were exposed to high titer phage lysates for isolation of resistant mutants. Using the soft agar overlay protocol described previously, host and phage were mixed at a MOI of 10 and poured onto MNBY plates. Plates were assessed daily for the development of phage resistant colonies. Colonies were streak purified a minimum of 3 times to dilute carryover phage. Putative resistant isolates were rechecked for phage

resistance by exposure to a phage dilution series. Randomly selected mutants were sequenced and compared with the wild type to determine what mutations in the chromosome were associated with phage resistance.

Bacterial genomic DNA extraction

ZR Fungal/Bacterial DNA MiniPrep Kit (Cat. No: D6005), Zymo Research, was used to extract bacterial genomic DNA. Briefly, bacterial cells from an overnight MNBY agar plate (~50-100 mg) were resuspended in 200 µl of distilled water and then added to ZR BashingBead Lysis Tube along with 750 µl of BashingBead buffer solution. The tubes were placed in the bead beater (Disruptor Genie), processed for 20 min and centrifuged at 10,000 x g at 25ºC for 1 min. Four hundred microliters of supernatant were transferred to a Zymo-Spin IV Spin Filter in a collection tube and centrifuged at 8,000 x g for 1 min at 25ºC. DNA extraction was completed by following the protocol according to the manufacturer and the DNA was stored at -20 ºC.

Bacterial whole genome sequencing and analysis

Bacterial DNA was sequenced using the Illumina MiSeq platform to generate paired-end 250 bp reads according to the manufacturer's guidelines. FastQC (bioinformatics.babraham.ac.uk), FastX Toolkit (hannonlab.cshl.edu), and SPAdes 3.5.0 (Bankevich et al., 2012) were used for read quality control, read trimming, and read assembly, respectively. The wild type and mutant genomes were assembled into contigs and then mapped to a close reference sequence *Xac* strain 306 (Accession: GCA_000007165.1). The tool BWA-MEM was used to map each bacterial strain's set of trimmed reads, both forwards and reverse, to the reference genome (Li, 2013; Li and Durbin, 2009, 2010). The result of BWA file could then be manually viewed using

Integrative genomics viewers (IGV) for further analysis (Robinson et al., 2011; Thorvaldsdóttir et al., 2013). In order to assess if the mutation that resulted in phage resistance was caused by a single nucleotide polymorphism (SNP) or an INDEL, we took the previously generated BWA files and applied the tool VarScan2 Call SNPs, Varscan2 Call INDELs (Koboldt et al., 2012). These tools were run on the default settings, which resulted in a number of calls that were of dubious quality. In order to remove the lower quality calls, we filtered the results using a Filter tool (VarScan) available in Galaxy. VarScan gave a binary value to each of the calls it provided for a number of parameters. One of these parameters was homozygosity. We found that at the default value of 0.75, in the parameter, "VarScan: Minimum frequency to call homozygote" generated a binary indication of a quality dataset. Therefore, we sorted the generated INDEL and SNP data based on their homozygous score, with 2s being quality (homozygous) and 0s (non-homozygous) being not quality. Using this filter made the output manually manageable. We manually analyzed the INDELs and SNPs to confirm in which gene the mutation had occurred and whether the associated changes resulted in a silent, nonsense, or missense mutation. Additionally, since this was a computationally annotated reference genome, we used NCBI BLAST and InterProScan to compare the gene homology if the reference genome had an undescriptive gene name (Altschul et al., 1990; Camacho et al., 2009; Jones et al., 2014).

Microtiter assay for growth study

A single colony in overnight broth culture of wild type and mutants were diluted and adjusted to OD_{600} = 1.0 (~ 10^9 CFU/ml) spectrophotometrically with MNBY broth, then used as inoculum for loading into Falcon 96 well flat bottom plate (Corning, Cat. No.

351172). For each well, 180 µl of MNYB broth was added along with 20 µl of *Xac* wild type strain and the putative resistant mutants (~ 10^8 CFU/ ml final concertation). The plate was incubated at 28 ºC with double orbital shaking at 150 rpm in a Tecan Spark 10 M plate reader (Tecan Group Ltd., Männedorf, Switzerland). The growth was monitored at OD_{600} at 30 min intervals for 23 h. After baseline adjustment, growth curves were generated by plotting OD_{600} measurements against time. All assays were done in triplicate.

Results and discussion

Deletion and complementation of *pilA*

A requirement of T4P has been observed for the infection of several members from the *Xanthomonadaceae* family including *Xanthomonas* and *Xylella fastidiosa* and members of the genus *Pseudomonas* (Ahern et al., 2014; Chibeu et al., 2009). Extensive research by several groups has been done to gain insights into the role played by T4P in bacteria-host interactions and pathogenesis, biofilm formation, twitching and sliding motility, and interactions with phages (Dunger et al., 2014; 2016). The T4P secretion machinery is made up of four subcomplexes: (i) the outer membrane subcomplex formed by the dodecameric ring of PilQ and the pilotin PilF, (ii) the inner membrane platform, made up of PilC, PilM, PilN, PilO and PilP, (iii) the ATPases PilB, PilT and PilU, and (iv) the pilus filament, a polymer of the major pilin, PilA, and minor pilins (Figure 10) (Dunger et al., 2016).

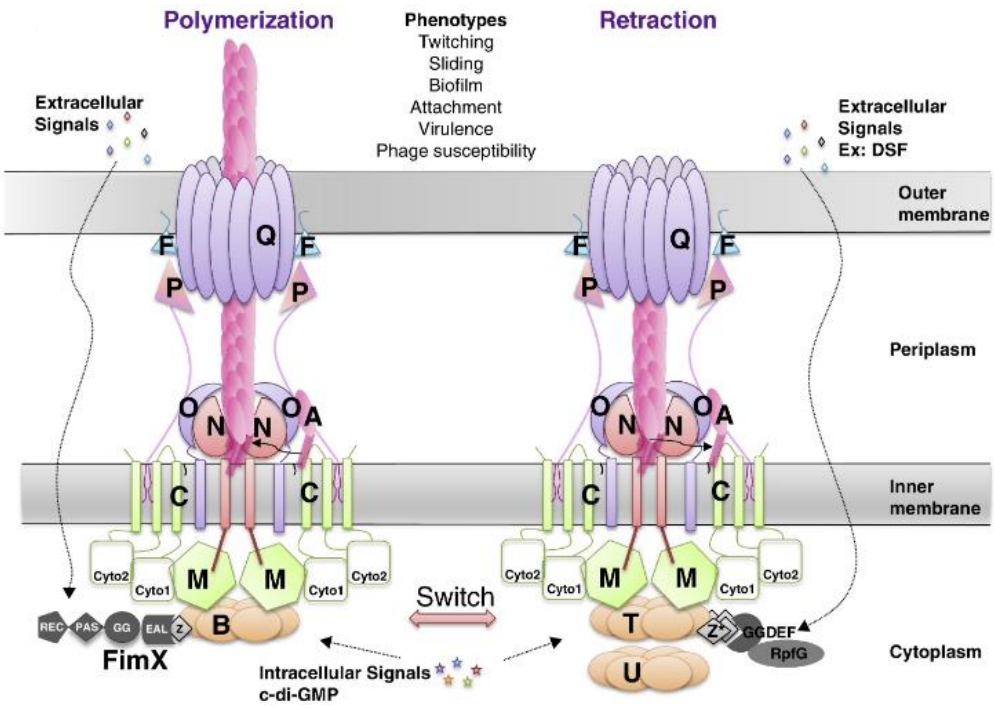

Figure 10. Type IV pilus machinery is made up of four subcomplexes: (i) the outer membrane subcomplex formed by the dodecameric ring of PilQ and the pilotin PilF, (ii) the inner membrane platform, made up of PilC, PilM, PilN, PilO and PilP, (iii) the ATPases PilB, PilT and PilU, and (iv) the pilus filament, a polymer of the major pilin, PilA, and minor pilins (Figure adapted from Dunger et al., 2016, with permission).

Xac strain 306 (the reference genome in this studied) was sequenced and fully annotated. Its genome contains genes with all necessary components for a functional T4P (da Silva et al., 2002). Figure 11 shows the T4P genes cluster.

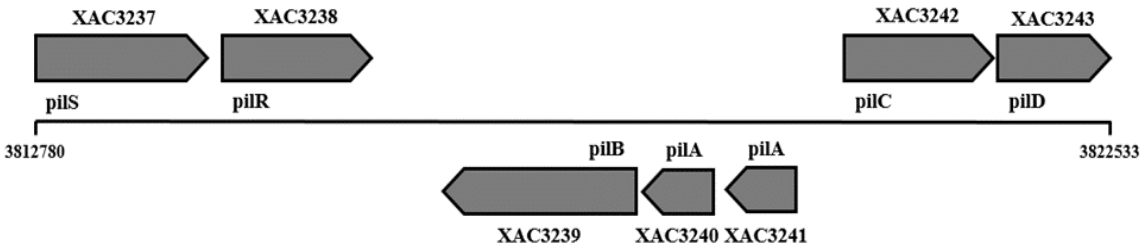

Figure 11. *Xac* 306 type IV pilus genes cluster.

We chose to delete *pilA*$_{XAC3241}$ in this study. As shown in Figure 11, the *pilA* genes (*pilA*$_{XAC3240}$ and *pilA*$_{XAC3241}$*)* are clustered with the other T4P-related genes *pilS*, *pilR*, *pilB*, *pilC*, and *pilD*. Previous studies showed while these two genes shared 67.6% amino acid sequences identity *pilA*$_{XAC3241}$ was more conserved among the *Xanthomonadaceae* family compared with its adjacent downstream homolog (Dunger et al., 2014; Dunger et al., 2016). Dunger at al. (2014) also showed that *pilA*$_{XAC3241}$ was expressed at a significantly greater level than *pilA*$_{XAC3240}$ and *XAC3805* (minor pilin) in liquid culture and at all time points after infiltration into host plants.

An in-frame deletion of *pilA* mutant was generated and complemented *in-trans* to examine the effect of the *pilA* mutation on plaque production. It was observed that Block 22 was sensitive to all the selected phages, whereas Block 22-*ΔpilA* was insensitive to all three phages CCP504, CCP513, and CCP509. However, sensitivity to the selected phages was restored when the pilA protein was restored *in-trans* (Table 11).

Table 11. Phage sensitivity testing of Block 22, *ΔpilA* mutant and complement.

Phage ID (morphology)	**Block 22**	**Block 22-*ΔpilA***	**Block 22-Comp**
CCP504 (Podo)	+[a]	-	+
CCP513 (Sipho)	+	-	+
CCP509 (Myo)	+	-	+

[a] Ability to form individual plaques on indicated host

Phage resistant mutant analysis by whole genome comparisons

Spontaneous phage resistance mutants also were selected to determine if other mutations could confer phage resistance, and thus identify other possible receptor(s). Four spontaneous phage resistant mutants were selected for whole genome sequencing along

with Block 22 (parental strain). Since *Xac* strain Block 22 was not sequenced previously, we used the fully annotated Xac 306 genome (Accession: GCA_000007165.1) as reference.

Our analysis found 14 INDELs and 268 SNPs among the four resistant mutants that were sequenced. After manually evaluation, it was determined that mutations occurred in both coding and non-coding regions. The INDELs were found mostly in the non-coding region, with the exception of one each in dipeptidyl anminopeptidase (XAC0262), cointegrate resolution protein T, *orfT*, (XAC3229) and *pilR* (XAC3238). The SNPs were found in hypothetical proteins such as XAC0123, XAC1346, XAC2251, and XAC3502. SNPs were also identified in functional genes such as the outer membrane component of a multidrug efflux pump (XAC1526), chemotaxis protein (XAC 1896), succinate dehydrogenase flavoprotein subunit (XAC2077), htpG heat shock protein G (XAC2528), Acyl-CoA dehydrogenase (XAC3054), *pilT* (XAC2924), *pilB* (XAC3239) and *orfT* and *orfS* (XAC3227). A SNP was identified in gene encoding for the outer membrane component of a multidrug efflux pump (XAC1526). However, the mutation in XAC1526 was determined to be a silent, because the SNP from T to G at 1761903 kb did not result in a change to the amino acid sequence of the protein. The SNP in *pilT* (mutant RC3) that replaced a G with T resulted in a missense mutation due to a one amino acid substitution (Gly to Val). In addition, a missense mutation was located in *pilB* (mutant RC4) that was due to a SNP from G to A resulted in the substitution of Asp to Glu. A frameshift mutation in *pilR* occurred due to a single base deletion. Thus, the *pilT* and *pilB* SNPs and the *pilR* INDEL were identified as mutation in the T4P gene cluster that would potentially affect the phage infection process (Table 12).

Table 12. Mutations associated with phage resistance to *Xac* type IV pilus dependent phage.

Genes in reference genome	Mutant strain	Position	Change	Mutation
XAC2924 - *pilT*	RC3	3431317	T	SNP from G to T (Gly to Val)
XAC3238 - *pilR*	RC4	3815895	+C	Single base insertion
XAC3239 - *pilB*	RC1, RC4, RC11	3818916	A	SNP from G to A (Asp to Glu)

The mutations were identified as possible receptor mutations because the mutations were localized in the T4P genes cluster (Figure 10 and 11). The *pilR*, *pilT* and *pilB* have important roles in T4P secretion machinery (Dunger et al., 2016). *PilR* is the response regulator in the two component system that controls transcription of the major pilin gene *pilA* (Hobbs et al., 1993). The binding of phosphorylated *pilR* to sequences upstream of the *pilA* promotor activates the transcription of *pilA* and results in the expression of pilin (Yang et al., 2004). Therefore, a mutation in *pilR* can lead to the down-regulation of *pilA*, which can lead to abolishment of phage infection of *Xac*. PilB utilizes the energy of ATP hydrolysis to catalyze the pilin subunits during pilus extension/polymerization, whereas pilT catalyzes the removal of pilus subunits during retraction/polymerization (Dunger et al., 2016). A mutation in *pilB* can result in resistance to a pilus-specific phage, as observed for phage PO4 (Nunn et al., 1990; Turner et al., 1993). A knockout of *pilB* abolishes T4P synthesis resulting in phage resistance. It also affects twitching motility and plant adherence in *Xanthomas* spp. (Dunger et al., 2014; Guzzo et al., 2009). Previous studies showed that *pilT* mutants are hyperpiliated but are deficient in pilus retraction (Bertrand et al., 2010; Graupner et al., 2001; Okamoto and Ohmori, 2002; Whitchurch and Mattick, 1994), which suggested that pilus retraction is essential for phage infection.

One of the challenges of phage therapy is the emergence of phage resistant mutants. However, in the case where T4P is the primary receptor, a mutation in an associated gene that results in impaired or no pilus function can have multiple effects on the bacterial host. Lack of pilus function can affect the fitness of the bacterium because of the role of function T4P in surface attachment, biofilm formation, and cell-to-cell aggregation (Dunger et al., 2014; Su et al., 1999; Yang et al., 2004). In *in vitro* studies, it was observed that phage resistant mutants exhibited reduced growth as compared to the wild type strain (Figure 12) indicating the loss of fitness associated with phage resistance.

In future studies, we would like to complement the *pilT*, *pilB* and *pilR* mutants to test their ability to restore phage sensitivity, and we would also like to test the pathogenicity of these mutants on host plants to further understand the fitness costs associated with the loss of the T4P system.

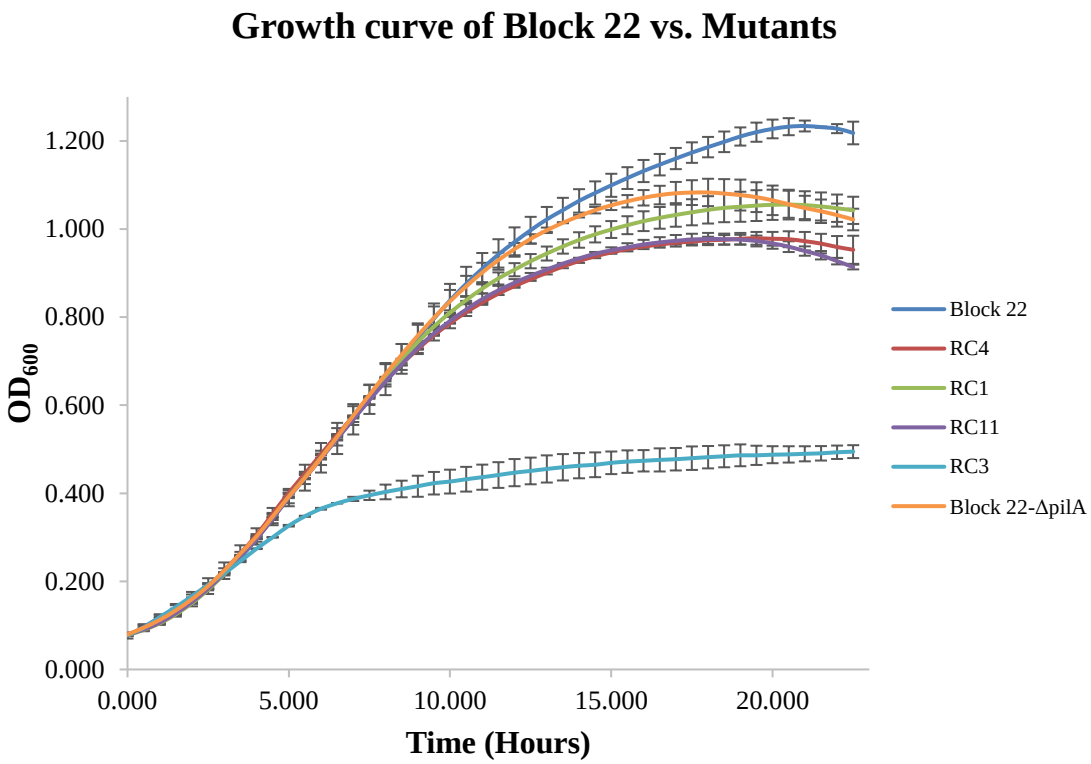

Figure 12. Growth defects associated with phage resistant mutants. The experiments were performed in triplicate, bars indicate standard deviation.

CHAPTER IV

EFFICACY STUDIES OF PHAGES COCKTAIL TO REDUCE CANKER SYMPTOMS IN GREENHOUSE TRIALS

Introduction

A biocontrol agent(s) can be used to prevent (prophylactic treatment) or treat (therapeutic treatment) disease. For prophylactic treatment, the phage cocktail is applied prior to the arrival of the pathogen. For therapeutic treatment, the phage cocktail would be introduced soon after the infection process has occurred, with the purpose of reducing the population in infected tissue to reduce disease severity (Svircev et al., 2018). Prevention is generally a better approach than treatment of the disease, but it is not always cost-efficient or possible. Citrus canker is primarily spread by wind and rain, therefore reducing the inoculum load is important in preventing disease spread. The efficacy of both options was evaluated as part of this biocontrol development. Since *Xac* naturally enters the leaf via stomatal openings, and then colonizes the apoplast, the phage and bacteria were sprayed specifically onto the leaves in greenhouse studies. All greenhouse experiments were conducted in cooperation with Dr. Nian Wang (Citrus Research and Education Center in Lake Alfred, FL). In Chapters II and III, I presented data on the isolation and characterization of *Xac* phages, with focus on phages CCP504, CCP509 and CCP513. Since the efficacy studies were conducted before full characterization of the phages could be completed, four phages were chosen for the greenhouse studies based on morphology, host range and preliminary annotation of sequenced genomes. The phages evaluated, as a

cocktail, in efficacy studies were three KMV-like podophages (CCP504, CCP505 and CCP511) and one siphophage (CCP513).

Materials and methods

Bacterial strain and phages

The canker bacterium *Xac* used in this study was stored at −80º C in nutrient broth (NB) (BBL, Becton Dickinson and Co., Cockeysville, MD) with 25% glycerol. For all experiments, the bacterial strain was grown on nutrient agar (NA) medium (BBL, Becton Dickinson and Co.) at 28º C. For preparation of bacterial suspensions, 36 h cultures were suspended in sterile tap water (STW), the concentration adjusted to 5×10^8 CFU/ml, and diluted appropriately. Bacteriophages used in this study were stored at 4°C in the dark. The phage cocktail used in plant trials was composed of three KMV-like podophages (CCP504, CCP505 and CCP511) and one siphophage (CCP513). The cocktail was an equal mixture of each of the phages with a final titer of 1×10^{10} PFU/ml and was diluted to desired concentrations in STW for greenhouse trials.

Plant greenhouse assays

Twenty week old Hamlin sweet orange plants were grown in 25-cm plastic pots in Fafard Professional Potting Mix (Sun Gro Horticulture, Agawam, MA) in a citrus canker quarantine greenhouse at 25 to 30°C in Lake Alfred, FL. The plants were watered every other day with tap water and fertilized with Peter professional ® 20-10-20 general purpose fertilizer (ICL Specialty Fertilizers, Dublin, Ohio) every seven days. The greenhouse (plastic roof, partially clear but not completely clear) received natural sunlight and no artificial light during the assays. The plants were heavily trimmed and fertilized to induce a new flush of growth. Approximately three weeks later, the emerging foliage were used for

inoculation. The inoculation was performed by a spray method with a hand-held 200 ml plastic spray bottle. The bottle was sterilized with 70% ethanol and washed with sterile tap water before use. Briefly, the abaxial surfaces of fully expanded, immature leaves of each plant were sprayed with a 20 ml aliquot of the following treatments: *Xac* only (disease control), phage cocktail only (phage control), phage (pre-phage treatment) followed by *Xac* 6 h later, or *Xac* inoculated 6 h prior to phage treatment (post-*Xac* treatment). Sterile tap water was used as a non-treament control. *Xac* strain Block 22 was used for inoculation of plants. Block 22 was grown on NA medium at 28°C for 36 h. A suspension of Block 22 was made in STW and adjusted spectrophotometrically to OD_{600} =0.5 (~ 5 x 10^8 CFU/ml). The suspension was serially diluted and plated on Nutrient Agar plates and incubated at 28°C for 48 h to confirm actual CFU/ml. In the first set of experiments, *Xac* suspension was diluted in STW to 5 x 10^6 CFU/ml and phages cocktail to 10^8 PFU/ml (MOI=20) for application; for the second set of experiments, *Xac* was applied at 5 x 10^8 CFU/ml and phages cocktail at 10^{10} PFU/ml (MOI=20). Silwett-L77 (silicone-polyether copolymer, Fisher Scientific), a wetting agent for increasing inoculum penetration, was used in each treatment at a 0.025% (vol/vol) final concentration. After inoculation, the plants were covered with white plastic bags for 24 h and then kept in the greenhouse (approximately 60% relative humidity). All inoculations included a minimum of three leaves at a similar developmental stage from each plant, and each treatment comprised five plants. Canker symptom progression was monitored phenotypically and the *Xac* population on inoculated leaves was estimated. In brief, three leaf discs randomly selected from each of two inoculated leaves were collected with a cork borer (0.8 cm in diameter) and ground in 1 ml of STW. The suspensions were serially diluted and plated on nutrient agar plates

containing the appropriate antibiotics. After incubation at 28° C for 48 h, bacterial colonies were counted and the number of CFU per square centimeter of leaf tissue was calculated. The experiments were repeated two times.

Results and discussion

In both sets of experiments, when the phage cocktail was applied either prior to or after the inoculation of *Xac*, the development of canker symptoms on Hamlin sweet orange leaves was reduced as compared to the disease control (*Xac* inoculation alone), as evidenced by reduced lesion numbers developed on the leaves surfaces (Figure 13). In the first set of experiments, where the phage mixture (10^8 PFU/ml) and *Xac* inoculum (5x 10^6 CFU/ml) were applied, the pre-*Xac* treatment showed better canker control than the post-*Xac* treatment with fewer lesion formations on the leaves' surfaces. The mean reductions in lesion formations were 52.7% and 47.4%, respectively (Table 13). In the second set of experiments, where the phage mixture (10^{10} PFU/ml) and *Xac* inoculum (5x 10^8 CFU/ml) were applied, the pre-*Xac* treatment and post-*Xac* treatment exhibited a similar control of canker symptoms, with a mean reduction in lesions formation of 42% and 44.9% respectively (Table 13).

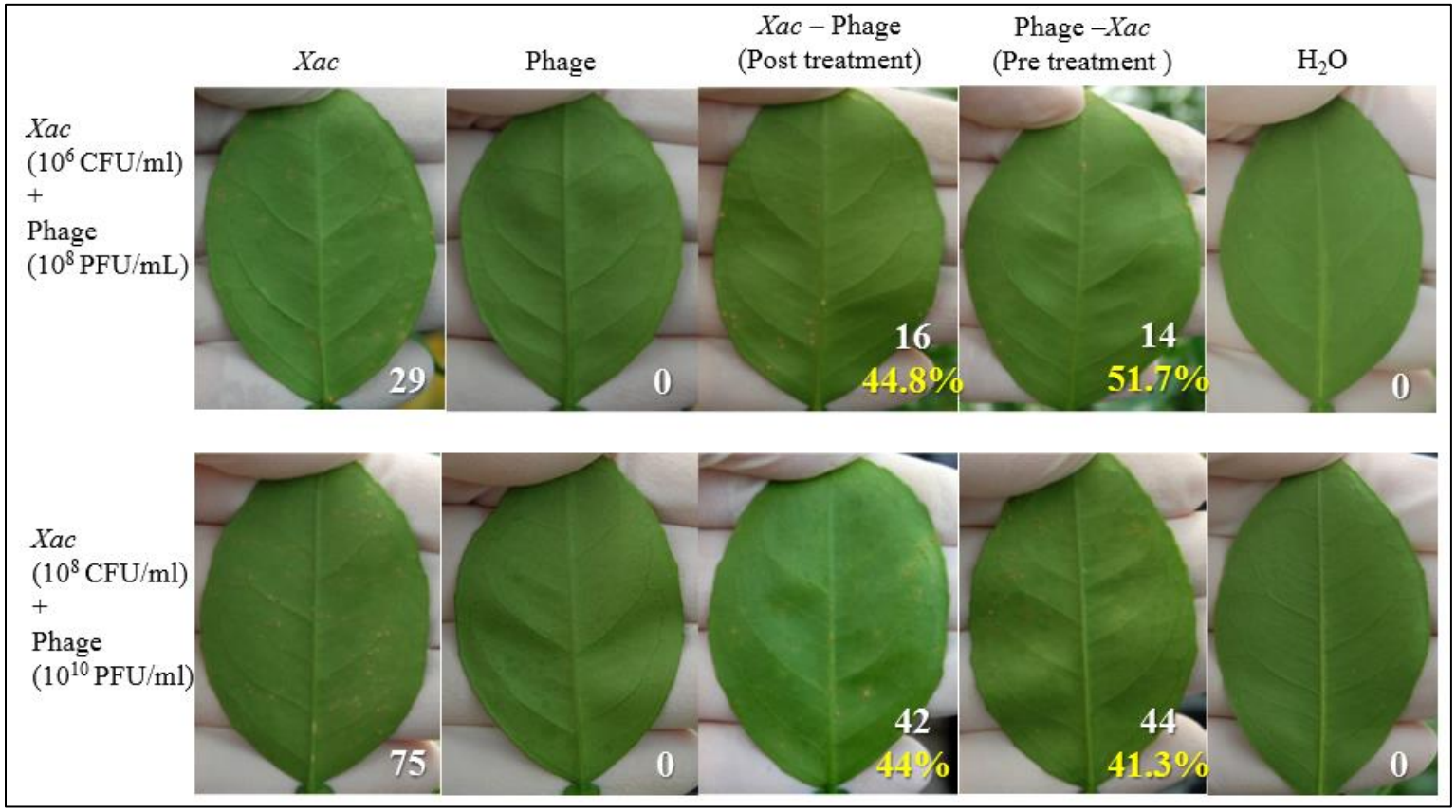

Figure 13. Effect of phage treatments on *Xac* infection on citrus leaves in greenhouse. Phage treatments reduced canker symptom development on Hamlin sweet orange leaves spray-inoculated by *Xac* (10^6 CFU/ml, up panel; and10^8 CFU/ml, down panel). Images are representative of five independent replicates at 21 days post inoculation. *Xac*: *Xac* mixed with sterile tap water alone (disease control); Phage: the phage mixture (10^8 PFU/ml or 10^{10} PFU/ml) inoculated alone (phage control); *Xac* - Phage: *Xac* inoculated 6 h before phage application (post-*Xac* treatment); Phage - *Xac*: phage applied 6 h before *Xac* inoculation (pre-*Xac* treatment), H_2O: sterile tap water alone.

Table 13. Suppression of bacterial canker formation on Hamlin sweet orange by phage treatment.

Treatment[a]	**Experiment #1**		**Experiment #2**		**Mean Reduction**
	Lesions/leaf[b]	**Reduction**[c]	**Lesions/leaf**	**Reduction**	
Xac (10^6 CFU/ml) (disease control)	29 ± 5	-	26 ± 6	-	-
Xac (10^6 CFU/ml) –Phage (10^8 PFU/ml) (post-*Xac* treatment)	16 ± 4	44.8%	13 ± 3	50%	47.4%
Phage (10^8 PFU/ml) –*Xac* (10^6 CFU/ml) (pre-*Xac* treatment)	14 ± 4	51.7%	12 ± 4	53.8%	52.7%
Xac (10^8 CFU/ml) (disease control)	75 ± 12	-	84 ± 15	-	-
Xac (10^8 CFU/ml) –Phage (10^{10} PFU/ml) (post-*Xac* treatment)	42 ± 7	44%	45 ± 8	45.8%	44.9%
Phage (10^{10} PFU/ml) –*Xac* (10^8 CFU/ml) (pre-*Xac* treatment)	44 ± 9	41.3%	48 ± 8	42.8%	42.0%

[a] Treatments were applied to Hamlin sweet orange plants. *Xac* - phage: phage treated 6 h –post *Xac* inoculation (post-*Xac* treatment); Phage - *Xac*: phage applied 6 h –prior to *Xac* inoculation (pre-*Xac* treatment).

[b] Lesion number assessed 21 days after inoculation with the pathogen. An average lesion number of five leaves was recorded.

[c] Lesion reduction (%) compared to the disease control.

We also monitored the effect of phage treatments on the growth of *Xac* populations in host plants. In the first set of experiments (5x 10^6 CFU/ml *Xac* inoculum), the populations of *Xac* recovered from pre-phage treatment and post-*Xac* treatment were approximately 10-fold and 5-fold fewer in CFU per square centimeter of leaf tissues than the disease control from 14 to 21 days post inoculation, respectively (Figure 14a). In the second set of experiments (5x 10^8 CFU/ml *Xac* inoculum), the populations of *Xac* recovered from both pre-*Xac* and post-*Xac* treatments were approximately 7-fold less in CFU per square centimeter of leaf tissues than the disease control at 21 days post inoculation (Figure 14b). There was an observed reduction in bacterial population from day 0 to 3 in phage treated (pre-*Xac* or post –*Xac*) plant tissue inoculated with 10^6 or 10^8 CFU/ml as compared with the *Xac* inoculated untreated plants. This drop in the initial population is also reflected in the lower number of lesions of leaves in treated plants (Table 13). The observed increase at both levels of inoculation after 3 days is likely due to the *Xac* population that entered the mesophyll through the stomata that were not exposed to the phage treatment. However, *Xac* population in pre or post – treatment plant tissue did not reach the same level as untreated over a 21-day period (Figure 14a and b)

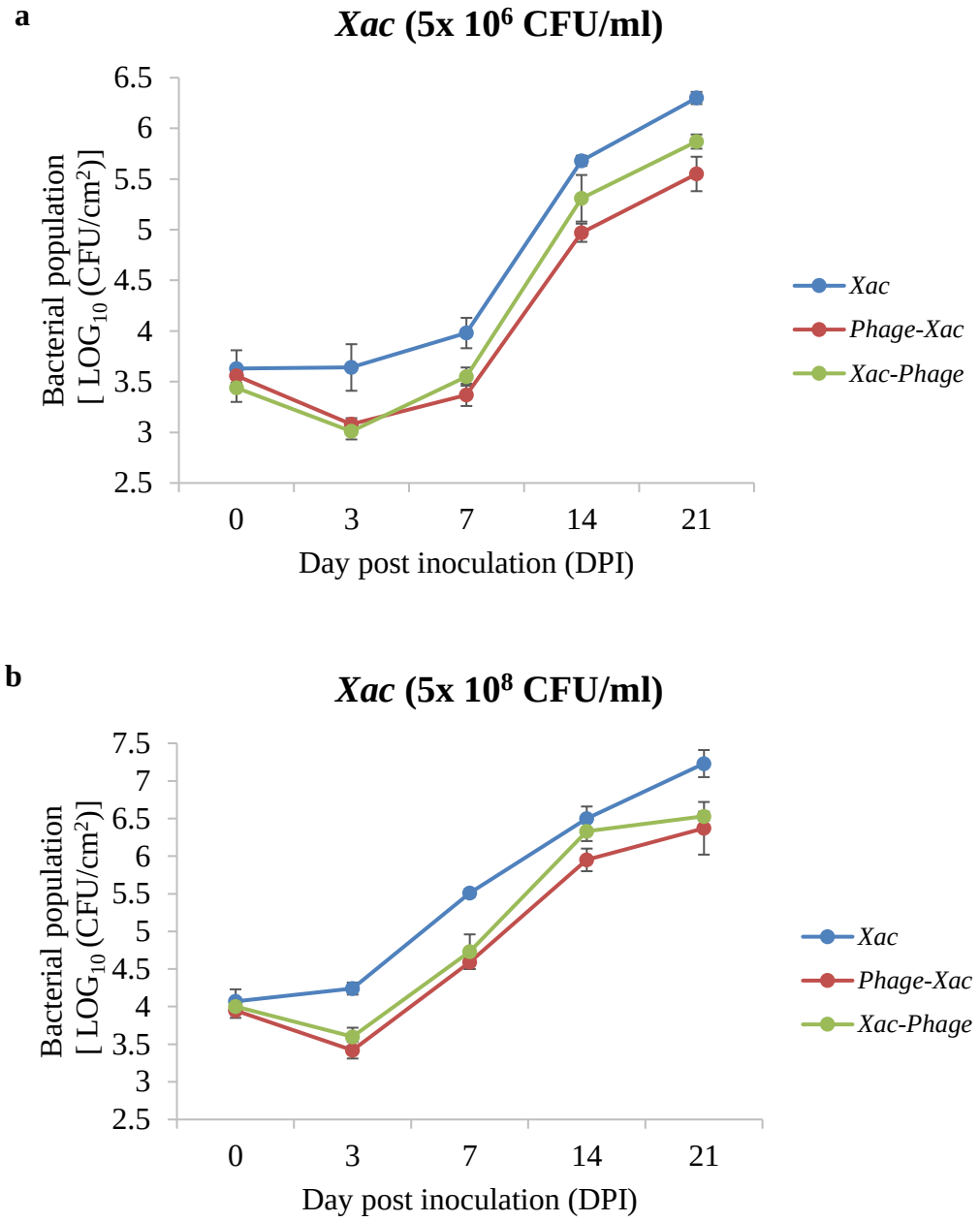

Figure 14. Phage treatments affected the growth of *Xac* populations on Hamlin sweet orange leaves following spray inoculation: (a) 10^6 CFU/ml, (b) 10^8 CFU/ml. Phage cocktail treatments were applied at and MOI of 20 for plant inoculated at both inoculum concentrations. Bacterial cells were recovered from the leaves at different time points after inoculation and quantified using the standard serial diluting-plating method. The values shown are means of six repeats and standard deviations. All the assays were repeated two times with similar results, bars indicate standard deviation.

The results of the growth of *Xac* populations in host plants in Figure 14 correlated with the results of lesion formation on the leaves surfaces showed in Table 13. Using JMP® Pro v14 (SAS Inst. Inc., Cary, NC, USA), the output of means comparisons for all pairs using Tukey-Kramer HSD ($p < 0.05$) showed that both phage treatments exhibited a statistically significant reduction of lesion formation compared to *Xac* inoculation alone; but there was not a statistical difference between the pre-*Xac* or post-*Xac* treatments (Table 14). With one treatment in a 21-day period, we confirmed the efficacy of the phage cocktail in reducing canker symptoms in greenhouse trials.

Table 14. Effect of phages cocktail treatments on canker symptoms development incited by Block22 in greenhouse trials.

Replicate		**Means of lesions formation**[a]			**p**[b]
	Block 22 concentration	**Disease control**	**Post-*Xac* treatment**	**Pre-*Xac* treatment**	
Experiment #1	10^6 CFU/ml	29a	16b	14b	0.0110
	10^8 CFU/ml	75a	42b	44b	0.0093
Experiment #2	10^6 CFU/ml	26a	13b	45b	0.0156
	10^8 CFU/ml	84a	12b	48b	0.0080

[a] Means within the same row followed by the same letter are not significantly different according to the Tukey-Kramer HSD multiple comparisons test in JMP® Pro v14, at p = 0.05 level.
[b] p = Probability that there are no differences in treatment means according to analysis of variance.

CHAPTER V

CONCLUSIONS AND FUTURE DIRECTIONS

The genus *Xanthomonas* is comprised of 27 species that can cause serious diseases in ~400 plant hosts, including a wide variety of economically important crops, such as rice, citrus, banana, cabbage, tomato, pepper and bean (Ryan et al., 2011). The goal of my study was to isolate virulent bacteriophages that could be used as biocontrol agents for the treatment of citrus canker caused by *Xac* as an alternative to copper sprays that have a negative impact on the plant health and the environment.

In this study, I isolated and purified 39 phages from environmental samples that formed plaques on *Xac* strains tested (Chapter II). In depth genomic characterization was conducted of three morphologically distinct *Xac* phages that exhibited different host ranges. Phage CCP504, a podophage, was determined to be phiKMV-like, since it contains a single subunit RNAP at the end of class II gene cluster of DNA metabolism and the metabolism genes follow the order of phiKMV-like phages and therefore a virulent, since all known KMV-like phages are virulent. Annotation of the siphophage CCP513 genome revealed that belonged to a novel phage type, whereas phage CCP509 was T4-like and virulent. All three phages were determined to utilize type IV pili as their primary receptor for infection process. Additionally, genomic analysis of spontaneous phage resistant *Xac* isolates determine that a mutation in *pilT*, *pilR* or *pilB* resulted in phage resistance due to abolishment or loss of function of the T4P. In *in vitro* studies, it was observed that phage resistant mutants exhibited reduced growth as compared to the wild type strain, indicating a loss of fitness associated with phage resistance (Chapter III).

Greenhouse studies were conducted to determine the efficacy of both prophylactic and therapeutic treatment with a phage cocktail composed of three KMV-like podophages (CCP504, CCP505 and CCP511) and one siphophage (CCP513). A significant reduction in lesion formation on leaves of Hamlin sweet orange plants was observed for both pre- and post-treated plants, as compared to non-treated. The growth of *Xac* population in host plants was also monitored to determine the effect of phage treatments. There was an observed reduction in bacterial population from day 0 to 3 in phage treated (pre-*Xac* or post-*Xac*) in plant tissue inoculated with at 10^6 or 10^8 CFU/ml as compared with the *Xac* inoculated untreated plants. Additionally, it was observed that the *Xac* population in pre or post-treatment plant tissue did not reach the same level as untreated over a 21-day period (Chapter IV).

Future studies should focus on the isolation of phages that are non-T4P dependent to expand the diversity of adsorption sites in the phage bank for future phage cocktail formulation. Additionally, greenhouse as well as field trials should be conducted to determine the optimal phage concentration and frequency of phage application to obtain maximum control of disease.

REFERENCES

Abedon, S.T., 2009. Kinetics of phage-mediated biocontrol of bacteria. Foodborne pathogens and disease 6, 807-815.

Ackermann, H.-W., 2006. Classification of bacteriophages. The bacteriophages 635, 8-16.

Afgan, E., Baker, D., Batut, B., Van Den Beek, M., Bouvier, D., Čech, M., Chilton, J., Clements, D., Coraor, N., Grüning, B.A., 2018. The Galaxy platform for accessible, reproducible and collaborative biomedical analyses: 2018 update. Nucleic acids research 46, W537-W544.

Agrios, G.N., 1997. Plant diseases caused by prokaryotes: Bacteria and mollicutes, Plant Pathology Academic Press, San Diego, California pp. 412-413.

Ahern, S.J., Das, M., Bhowmick, T.S., Young, R., Gonzalez, C.F., 2014. Characterization of novel virulent broad-host-range phages of Xylella fastidiosa and Xanthomonas. Journal of bacteriology 196, 459-471.

Altschul, S.F., Gish, W., Miller, W., Myers, E.W., Lipman, D.J., 1990. Basic local alignment search tool. Journal of molecular biology 215, 403-410.

Bankevich, A., Nurk, S., Antipov, D., Gurevich, A.A., Dvorkin, M., Kulikov, A.S., Lesin, V.M., Nikolenko, S.I., Pham, S., Prjibelski, A.D., Pyshkin, A.V., Sirotkin, A.V., Vyahhi, N., Tesler, G., Alekseyev, M.A., Pevzner, P.A., 2012. SPAdes: a new genome assembly algorithm and its applications to single-cell sequencing. J Comput Biol 19, 455-477.

Barber, C., Tang, J., Feng, J., Pan, M., Wilson, T., Slater, H., Dow, J., Williams, P., Daniels, M., 1997. A novel regulatory system required for pathogenicity of Xanthomonas campestris is mediated by a small diffusible signal molecule. Molecular microbiology 24, 555-566.

Behlau, F., Belasque Jr, J., Bergamin Filho, A., Graham, J., Leite Jr, R., Gottwald, T., 2008. Copper sprays and windbreaks for control of citrus canker on young orange trees in southern Brazil. Crop Protection 27, 807-813.

Behlau, F., Fonseca, A., Belasque Jr, J., 2016. A comprehensive analysis of the Asiatic citrus canker eradication programme in São Paulo state, Brazil, from 1999 to 2009. Plant Pathology 65, 1390-1399.

Behlau, F., Scandelai, L.H.M., da Silva Junior, G.J., Lanza, F.E., 2017. Soluble and insoluble copper formulations and metallic copper rate for control of citrus canker on sweet orange trees. Crop protection 94, 185-191.

Belasque Jr, J., Parra-Pedrazzoli, A., Rodrigues Neto, J., Yamamoto, P., Chagas, M., Parra, J., Vinyard, B., Hartung, J., 2005. Adult citrus leafminers (Phyllocnistis citrella) are not efficient vectors for Xanthomonas axonopodis pv. citri. Plant Disease 89, 590-594.

Bertani, G., 1951. Studies on lysogenesis I.: the mode of phage liberation by lysogenic Escherichia coli1. Journal of bacteriology 62, 293.

Bertozzi Silva, J., Storms, Z., Sauvageau, D., 2016. Host receptors for bacteriophage adsorption. FEMS Microbiology Letters 363.

Bertrand, J.J., West, J.T., Engel, J.N., 2010. Genetic analysis of the regulation of type IV pilus function by the Chp chemosensory system of Pseudomonas aeruginosa. Journal of bacteriology 192, 994-1010.

Brunings, A.M., Gabriel, D.W., 2003. Xanthomonas citri: breaking the surface. Molecular plant pathology 4, 141-157.

Brüssow, H., 2007. Bacteria between protists and phages: from antipredation strategies to the evolution of pathogenicity. Molecular microbiology 65, 583-589.

Brüssow, H., Canchaya, C., Hardt, W.-D., 2004. Phages and the evolution of bacterial pathogens: from genomic rearrangements to lysogenic conversion. Microbiol. Mol. Biol. Rev. 68, 560-602.

Brüssow, H., Hendrix, R.W., 2002. Phage genomics: small is beautiful. Cell 108, 13-16.

Buttimer, C., McAuliffe, O., Ross, R.P., Hill, C., O'Mahony, J., Coffey, A., 2017. Bacteriophages and bacterial plant diseases. Frontiers in microbiology 8, 34.

Camacho, C., Coulouris, G., Avagyan, V., Ma, N., Papadopoulos, J., Bealer, K., Madden, T.L., 2009. BLAST+: architecture and applications. BMC bioinformatics 10, 421.

Chaturongakul, S., Ounjai, P., 2014. Phage–host interplay: examples from tailed phages and Gram-negative bacterial pathogens. Frontiers in microbiology 5, 442.

Chibeu, A., Ceyssens, P.-J., Hertveldt, K., Volckaert, G., Cornelis, P., Matthijs, S., Lavigne, R., 2009. The adsorption of Pseudomonas aeruginosa bacteriophage φKMV is dependent on expression regulation of type IV pili genes. FEMS microbiology letters 296, 210-218.

Clokie, M.R., Millard, A.D., Letarov, A.V., Heaphy, S., 2011. Phages in nature. Bacteriophage 1, 31-45.

Cubero, J., Graham, J., 2002. Genetic relationship among worldwide strains of Xanthomonas causing canker in citrus species and design of new primers for their identification by PCR. Appl. Environ. Microbiol. 68, 1257-1264.

da Silva, A.C.R., Ferro, J.A., Reinach, F.C., Farah, C.S., Furlan, L.R., Quaggio, R.B., Monteiro-Vitorello, C.B., Sluys, M.A.V., Almeida, N.F., Alves, L.M.C., do Amaral, A.M., Bertolini, M.C., Camargo, L.E.A., Camarotte, G., Cannavan, F., Cardozo, J., Chambergo, F., Ciapina, L.P., Cicarelli, R.M.B., Coutinho, L.L., Cursino-Santos, J.R., El-Dorry, H., Faria, J.B., Ferreira, A.J.S., Ferreira, R.C.C., Ferro, M.I.T., Formighieri, E.F., Franco, M.C., Greggio, C.C., Gruber, A., Katsuyama, A.M., Kishi, L.T., Leite, R.P., Lemos, E.G.M., Lemos, M.V.F., Locali, E.C., Machado, M.A., Madeira, A.M.B.N., Martinez-Rossi, N.M., Martins, E.C., Meidanis, J., Menck, C.F.M., Miyaki, C.Y., Moon, D.H., Moreira, L.M., Novo, M.T.M., Okura, V.K., Oliveira, M.C., Oliveira, V.R., Pereira, H.A., Rossi, A., Sena, J.A.D., Silva, C., de Souza, R.F., Spinola, L.A.F., Takita, M.A., Tamura, R.E., Teixeira, E.C., Tezza, R.I.D., Trindade dos Santos, M., Truffi, D., Tsai, S.M., White, F.F., Setubal, J.C., Kitajima, J.P., 2002. Comparison of the genomes of two Xanthomonas pathogens with differing host specificities. Nature 417, 459-463.

Darling, A.C., Mau, B., Blattner, F.R., Perna, N.T., 2004. Mauve: multiple alignment of conserved genomic sequence with rearrangements. Genome research 14, 1394-1403.

Das, A., 2003. Citrus canker-A review. Journal of Applied Horticulture 5, 52-60.

de Leeuw, M., Baron, M., Brenner, A., Kushmaro, A., 2017. Genome Analysis of a Novel Broad Host Range Proteobacteria Phage Isolated from a Bioreactor Treating Industrial Wastewater. Genes 8, 40.

Delbrück, M., 1945. The burst size distribution in the growth of bacterial viruses (bacteriophages). Journal of bacteriology 50, 131.

Delcher, A.L., Harmon, D., Kasif, S., White, O., Salzberg, S.L., 1999. Improved microbial gene identification with GLIMMER. Nucleic acids research 27, 4636-4641.

Dewdney, M., Roberts, P., Graham, J., Chung, K., Zekri, M., Homeowner Fact Sheet: Citrus Canker1.

Doss, J., Culbertson, K., Hahn, D., Camacho, J., Barekzi, N., 2017. A review of phage therapy against bacterial pathogens of aquatic and terrestrial organisms. Viruses 9, 50.

Duan, Y., Castaneda, A., Zhao, G., Erdos, G., Gabriel, D., 1999. Expression of a single, host-specific, bacterial pathogenicity gene in plant cells elicits division, enlargement, and cell death. Molecular Plant-Microbe Interactions 12, 556-560.

Duckworth, D.H., 1976. " Who discovered bacteriophage?". Bacteriological reviews 40, 793.

Dunger, G., Guzzo, C.R., Andrade, M.O., Jones, J.B., Farah, C.S., 2014. Xanthomonas citri subsp. citri type IV pilus is required for twitching motility, biofilm development, and adherence. Molecular Plant-Microbe Interactions 27, 1132-1147.

Dunger, G., Llontop, E., Guzzo, C.R., Farah, C.S., 2016. The Xanthomonas type IV pilus. Current opinion in microbiology 30, 88-97.

Ference, C.M., Gochez, A.M., Behlau, F., Wang, N., Graham, J.H., Jones, J.B., 2018. Recent advances in the understanding of Xanthomonas citri ssp. citri pathogenesis and citrus canker disease management. Molecular plant pathology 19, 1302-1318.

Frampton, R.A., Pitman, A.R., Fineran, P.C., 2012. Advances in bacteriophage-mediated control of plant pathogens. International journal of microbiology 2012.

Garneau, J.R., Depardieu, F., Fortier, L.-C., Bikard, D., Monot, M., 2017. PhageTerm: a tool for fast and accurate determination of phage termini and packaging mechanism using next-generation sequencing data. Scientific reports 7, 8292.

Gill, J.J., Hyman, P., 2010. Phage choice, isolation, and preparation for phage therapy. Current pharmaceutical biotechnology 11, 2-14.

Goodwin, B.K., Piggott, N.E., 2006. Risk and indemnification models of infectious plant diseases.

Goto, M., Hyodo, H., 1985. Role of extracellular polysaccharides of Xanthomonas campestris pv. citri in the early stage of infection. Japanese Journal of Phytopathology 51, 22-31.

Gottig, N., Garavaglia, B., Garofalo, C., Zimaro, T., Sgro, G., Ficarra, F., Dunger, G., Daurelio, L., Thomas, L., Gehring, C., 2010. Mechanisms of infection used by Xanthomonas axonopodis pv. citri incitrus canker disease. Current Research, Technology and Education Topics in Applied Microbiology and Microbial Biotechnology 1, 196-204.

Gottwald, T., Timmer, L., 1995. The efficacy of windbreaks in reducing the spread of citrus canker caused by Xanthomonas campestris pv. citri. Tropical Agriculture 72, 194-201.

Gottwald, T.R., Graham, J.H., Schubert, T.S., 2002. Citrus canker: the pathogen and its impact. Plant Health Progress 10, 32.

Gottwald, T.R., Irey, M., 2007. Post-hurricane analysis of citrus canker II: predictive model estimation of disease spread and area potentially impacted by various eradication protocols following catastrophic weather events. Plant Health Progress 10.

Graham, J., Dewdney, M., Myers, M., 2010. Streptomycin and copper formulations for control of citrus canker on grapefruit, Proceedings of the Florida State Horticultural Society. Florida State Horticultural Society, pp. 92-99.

Graham, J., Gottwald, T., Civerolo, E., McGuire, R., 1989. Population dynamics and survival of Xanthomonas campestris in soil in citrus nurseries in Maryland and Argentina. Plant Disease (USA).

Graham, J.H., Gottwald, T.R., Cubero, J., Achor, D.S., 2004. Xanthomonas axonopodis pv. citri: factors affecting successful eradication of citrus canker. Molecular plant pathology 5, 1-15.

Graupner, S., Weger, N., Sohni, M., Wackernagel, W., 2001. Requirement of Novel Competence Genes pilT andpilU of Pseudomonas stutzeri for Natural Transformation and Suppression of pilT Deficiency by a Hexahistidine Tag on the Type IV Pilus Protein PilAI. Journal of bacteriology 183, 4694-4701.

Guzzo, C.R., Salinas, R.K., Andrade, M.O., Farah, C.S., 2009. PILZ protein structure and interactions with PILB and the FIMX EAL domain: implications for control of type IV pilus biogenesis. Journal of molecular biology 393, 848-866.

Hamad, M.A., Zajdowicz, S.L., Holmes, R.K., Voskuil, M.I., 2009. An allelic exchange system for compliant genetic manipulation of the select agents Burkholderia pseudomallei and Burkholderia mallei. Gene 430, 123-131.

He, S.Y., 1998. Type III protein secretion systems in plant and animal pathogenic bacteria. Annual review of phytopathology 36, 363-392.

Hobbs, M., Collie, E., Free, P., Livingston, S., Mattick, J., 1993. PilS and PilR, a two-component transcriptional regulatory system controlling expression of type 4 fimbriae in Pseudomonas aeruginosa. Molecular microbiology 7, 669-682.

Jones, P., Binns, D., Chang, H.-Y., Fraser, M., Li, W., McAnulla, C., McWilliam, H., Maslen, J., Mitchell, A., Nuka, G., 2014. InterProScan 5: genome-scale protein function classification. Bioinformatics 30, 1236-1240.

Kandeler, F., Kampichler, C., Horak, O., 1996. Influence of heavy metals on the functional diversity of soil microbial communities. Biology and fertility of soils 23, 299-306.

Koboldt, D.C., Zhang, Q., Larson, D.E., Shen, D., McLellan, M.D., Lin, L., Miller, C.A., Mardis, E.R., Ding, L., Wilson, R.K., 2012. VarScan 2: somatic mutation and copy number alteration discovery in cancer by exome sequencing. Genome research 22, 568-576.

Koizumi, M., Kochinotsu, B., 1977. Relation of temperature to the development of citrus canker lesions in the spring, Proc. Int. Soc. Citriculture, pp. 924-928.

Koskella, B., Taylor, T.B., 2018. Multifaceted impacts of bacteriophages in the plant microbiome. Annual review of phytopathology 56, 361-380.

Kuty, G.F., Xu, M., Struck, D.K., Summer, E.J., Young, R., 2010. Regulation of a phage endolysin by disulfide caging. Journal of bacteriology 192, 5682-5687.

Laslett, D., Canback, B., 2004. ARAGORN, a program to detect tRNA genes and tmRNA genes in nucleotide sequences. Nucleic acids research 32, 11-16.

Lavigne, R., Burkal'tseva, M.V., Robben, J., Sykilinda, N.N., Kurochkina, L.P., Grymonprez, B., Jonckx, B., Krylov, V.N., Mesyanzhinov, V.V., Volckaert, G., 2003. The genome of bacteriophage φKMV, a T7-like virus infecting Pseudomonas aeruginosa. Virology 312, 49-59.

Lee, E., Helt, G.A., Reese, J.T., Munoz-Torres, M.C., Childers, C.P., Buels, R.M., Stein, L., Holmes, I.H., Elsik, C.G., Lewis, S.E., 2013. Web Apollo: a web-based genomic annotation editing platform. Genome biology 14, R93.

Lee, J., Oh, J., Min, K.R., Kim, C.-K., Min, K.-H., Lee, K.-S., Kim, Y.-C., Lim, J.-Y., Kim, Y., 1996. Structure of Catechol 2, 3-Dioxygenase Gene Encoded in Chromosomal DNA ofPseudomonas putidaKF715. Biochemical and biophysical research communications 224, 831-836.

Leite Jr, R., Mohan, S., 1990. Integrated management of the citrus bacterial canker disease caused by Xanthomonas campestris pv. citri in the State of Paraná, Brazil. Crop Protection 9, 3-7.

Levin, B.R., Bull, J.J., 2004. Population and evolutionary dynamics of phage therapy. Nature Reviews Microbiology 2, 166.

Li, H., 2013. Aligning sequence reads, clone sequences and assembly contigs with BWA-MEM. arXiv preprint arXiv:1303.3997.

Li, H., Durbin, R., 2009. Fast and accurate short read alignment with Burrows–Wheeler transform. Bioinformatics 25, 1754-1760.

Li, H., Durbin, R., 2010. Fast and accurate long-read alignment with Burrows–Wheeler transform. Bioinformatics 26, 589-595.

Li, L., Li, J., Zhang, Y., Wang, N., 2019. Diffusible signal factor (DSF)-mediated quorum sensing modulates expression of diverse traits in Xanthomonas citri and responses of citrus plants to promote disease. BMC Genomics 20, 55.

Moschini, R.C., Canteros, B.I., Martínez, M.I., De Ruyver, R., 2014. Quantification of the environmental effect on citrus canker intensity at increasing distances from a natural windbreak in northeastern Argentina. Australasian plant pathology 43, 653-662.

Nobrega, F.L., Vlot, M., de Jonge, P.A., Dreesens, L.L., Beaumont, H.J., Lavigne, R., Dutilh, B.E., Brouns, S.J., 2018. Targeting mechanisms of tailed bacteriophages. Nature Reviews Microbiology, 1.

Noguchi, H., Taniguchi, T., Itoh, T., 2008. MetaGeneAnnotator: detecting species-specific patterns of ribosomal binding site for precise gene prediction in anonymous prokaryotic and phage genomes. DNA research 15, 387-396.

Nunn, D., Bergman, S., Lory, S., 1990. Products of three accessory genes, pilB, pilC, and pilD, are required for biogenesis of Pseudomonas aeruginosa pili. Journal of bacteriology 172, 2911-2919.

Okamoto, S., Ohmori, M., 2002. The cyanobacterial PilT protein responsible for cell motility and transformation hydrolyzes ATP. Plant and cell physiology 43, 1127-1136.

Parasion, S., Kwiatek, M., Gryko, R., Mizak, L., Malm, A., 2014. Bacteriophages as an alternative strategy for fighting biofilm development. Pol. J. Microbiol 63, 137-145.

Payne, R.J., Jansen, V.A., 2001. Understanding bacteriophage therapy as a density-dependent kinetic process. Journal of Theoretical Biology 208, 37-48.

Penadés, J.R., Chen, J., Quiles-Puchalt, N., Carpena, N., Novick, R.P., 2015. Bacteriophage-mediated spread of bacterial virulence genes. Current opinion in microbiology 23, 171-178.

Rakhuba, D., Kolomiets, E., Dey, E.S., Novik, G., 2010. Bacteriophage receptors, mechanisms of phage adsorption and penetration into host cell. Pol. J. Microbiol 59, 145-155.

Ritenour, M.A., Pilon, L., Muraro, R., Narciso, J., BURKS, T.F., 2010. Commercial Postharvest Practices Used to Handle Fresh Citrus Fruit with Canker Symptoms, Proc. Fla. State Hort. Soc, pp. 255-258.

Robinson, J.T., Thorvaldsdóttir, H., Winckler, W., Guttman, M., Lander, E.S., Getz, G., Mesirov, J.P., 2011. Integrative genomics viewer. Nature biotechnology 29, 24.

Ryan, R.P., An, S.-q., Allan, J.H., McCarthy, Y., Dow, J.M., 2015. The DSF family of cell–cell signals: an expanding class of bacterial virulence regulators. PLoS pathogens 11, e1004986.

Ryan, R.P., Vorhölter, F.-J., Potnis, N., Jones, J.B., Van Sluys, M.-A., Bogdanove, A.J., Dow, J.M., 2011. Pathogenomics of Xanthomonas: understanding bacterium–plant interactions. Nature Reviews Microbiology 9, 344.

Schmelcher, M., Loessner, M.J., 2014. Application of bacteriophages for detection of foodborne pathogens. Bacteriophage 4, e28137.

Schubert, T.S., Miller, J., 1996. Bacterial citrus canker. Fla. Department Agric. & Consumer Services, Division of Plant Industry.

Schubert, T.S., Rizvi, S.A., Sun, X., Gottwald, T.R., Graham, J.H., Dixon, W.N., 2001. Meeting the challenge of eradicating citrus canker in Florida—again. Plant disease 85, 340-356.

Schwartz, M., 1975. Reversible interaction between coliphage lambda and its receptor protein. Journal of molecular biology 99, 185-201.

Skurnik, M., Strauch, E., 2006. Phage therapy: facts and fiction. International Journal of Medical Microbiology 296, 5-14.

Stein, B., Ramallo, J., Foguet, L., Graham, J.H., 2007. REFEREED MANUSCRIPT, Proc. Fla. State Hort. Soc, pp. 127-131.

Su, W.-C., Tung, S.-Y., Yang, M.-K., Kuo, T.-T., 1999. The pilA gene of Xanthomonas campestris pv. citri is required for infection by the filamentous phage cf. Molecular and General Genetics MGG 262, 22-26.

Summer, E.J., Enderle, C.J., Ahern, S.J., Gill, J.J., Torres, C.P., Appel, D.N., Black, M.C., Young, R., Gonzalez, C.F., 2010. Genomic and biological analysis of phage Xfas53 and related prophages of Xylella fastidiosa. Journal of bacteriology 192, 179-190.

Svircev, A., Roach, D., Castle, A., 2018. Framing the future with bacteriophages in agriculture. Viruses 10, 218.

Thorvaldsdóttir, H., Robinson, J.T., Mesirov, J.P., 2013. Integrative Genomics Viewer (IGV): high-performance genomics data visualization and exploration. Briefings in bioinformatics 14, 178-192.

Timmer, L., Gottwald, T., Zitko, S., 1991. Bacterial exudation from lesions of Asiatic citrus canker and citrus bacterial spot. Plant disease (USA).

Turner, L., Lara, J.C., Nunn, D., Lory, S., 1993. Mutations in the consensus ATP-binding sites of XcpR and PilB eliminate extracellular protein secretion and pilus biogenesis in Pseudomonas aeruginosa. Journal of bacteriology 175, 4962-4969.

Valentine, R.C., Shapiro, B., Stadtman, E., 1968. Regulation of glutamine synthetase. XII. Electron microscopy of the enzyme from Escherichia coli. Biochemistry 7, 2143-2152.

Vidaver, A.M., 1967. Synthetic and complex media for the rapid detection of fluorescence of phytopathogenic pseudomonads: effect of the carbon source. Papers in Plant Pathology, 59.

Whitchurch, C.B., Mattick, J.S., 1994. Characterization of a gene, pilU, required for twitching motility but not phage sensitivity in Pseudomonas aeruginosa. Molecular microbiology 13, 1079-1091.

White, T.J., Gonzalez, C.F., 1995. Electroporation of Xanthomonas, Electroporation Protocols for Microorganisms. Springer, pp. 135-141.

Xu, J., Hendrix, R.W., Duda, R.L., 2004a. Conserved translational frameshift in dsDNA bacteriophage tail assembly genes. Molecular cell 16, 11-21.

Xu, M., Struck, D.K., Deaton, J., Wang, N., Young, R., 2004b. A signal-arrest-release sequence mediates export and control of the phage P1 endolysin. Proceedings of the National Academy of Sciences of the United States of America 101, 6415-6420.

Yang, Y.-C., Chou, C.-P., Kuo, T.-T., Lin, S.-H., Yang, M.-K., 2004. PilR enhances the sensitivity of Xanthomonas axonopodis pv. citri to the infection of filamentous bacteriophage Cf. Current microbiology 48, 251-261.

Yarmolinsky, M.B., Sternberg, N., 1988. Bacteriophage P1, in: Calendar, R. (Ed.), The Bacteriophages. Springer US, Boston, MA, pp. 291-438.

Zhou, X., He, Z., Liang, Z., Stoffella, P.J., Fan, J., Yang, Y., Powell, C.A., 2011. Long-term use of copper-containing fungicide affects microbial properties of citrus grove soils. Soil Science Society of America Journal 75, 898-906.